

SOME ASPECTS OF THREE-DIMENSIONAL  
COANDA PHENOMENON

by

Donald Ray Bausler

---

A Thesis Submitted to the Faculty of the  
DEPARTMENT OF AEROSPACE ENGINEERING  
In Partial Fulfillment of the Requirements  
For the Degree of  
MASTER OF SCIENCE  
In the Graduate College  
THE UNIVERSITY OF ARIZONA

1 9 6 5

STATEMENT BY AUTHOR

This thesis has been submitted in partial fulfillment of requirements for an advanced degree at The University of Arizona and is deposited in the University Library to be made available to borrowers under rules of the Library.

Brief quotations from this thesis are allowable without special permission, provided that accurate acknowledgment of source is made. Request for permission for extended quotation from or reproduction of this manuscript in whole or in part may be granted by the head of the major department or by the Dean of the Graduate College when in his judgment the proposed use of the material is in the interests of scholarship. In all other instances, however, permission must be obtained from the author.

SIGNED: *Donald R. Bauster*

APPROVAL BY THESIS DIRECTOR

This thesis has been approved on the date shown below:

*E. K. Parks*  
E. K. PARKS  
Professor of Mechanical Engineering  
(Aerospace)

*5/5/65*  
Date

## ACKNOWLEDGMENT

The author is deeply grateful to Dr. E. K. Parks. His suggestion of the project and his subsequent guidance and inspiration made this investigation possible.

The author also sincerely appreciates the invaluable assistance of Professor A. G. Foster for his technical advice and guidance in fabricating the test apparatus. Further thanks are due to Mr. O. B. O'Brien for his assistance in machining the nozzle; Mrs. Newton, Technical Library, Fort Huachuca, Arizona, for securing the literature surveyed; Major F. J. Palermo for his cooperation in making available for comparison his data on two-dimensional Coanda flow; and to Mrs. Meta Anderson for typing this study.

## TABLE OF CONTENTS

	Page
ILLUSTRATIONS . . . . .	vi
SYMBOLS . . . . .	viii
ABSTRACT . . . . .	x
I INTRODUCTION . . . . .	1
1.1 General . . . . .	1
1.2 Historical Development . . . . .	7
1.3 Chronological Review of the Literature . . . . .	10
1.4 Purpose of the Study . . . . .	22
II THEORETICAL CONSIDERATIONS . . . . .	23
2.1 General . . . . .	23
2.2 Three-Dimensional Flow . . . . .	26
III TEST APPARATUS AND DATA MEASURING EQUIPMENT . . . . .	31
3.1 Test Apparatus . . . . .	31
3.1.1 Air Supply . . . . .	34
3.1.2 Air Bearings . . . . .	34
3.1.3 Plenum Chamber . . . . .	37
3.1.4 Three-Dimensional Coanda Nozzle . . . . .	37
3.1.5 Throttling Valve . . . . .	41
3.2 Data Measuring Equipment . . . . .	41
3.2.1 Manometers . . . . .	42

	Page
3.2.2 Surface Pressure Measurement . . .	42
3.2.3 Total and Static Pressure Measure- ment in the Coanda Sheet . . . . .	43
3.2.4 Total Pressure Measurement in the Plenum Chamber . . . . .	44
3.2.5 Horizontal and Vertical Force Measurement . . . . .	44
3.2.6 Flow Visualization . . . . .	46
IV TEST PROCEDURE AND DATA ANALYSIS . . . . .	48
4.1 General . . . . .	48
4.2 Surface Pressure Distribution . . . . .	48
4.3 Velocities and Thickness of the Coanda Sheet . . . . .	55
4.4 Forces Produced by Coanda Flow . . . . .	62
V CONCLUSIONS . . . . .	74
5.1 Conclusions . . . . .	74
5.2 Recommendations for Further Research . . .	76
REFERENCES . . . . .	78

## ILLUSTRATIONS

Figure	Page
1. Basic "Coanda Effect" Nozzle . . . . .	2
2. Induced Flow Nozzle . . . . .	2
3. High-Lift, Low-Drag Wing . . . . .	4
4. Handley Page Wing . . . . .	4
5. Wind Tunnel Fan . . . . .	6
6. Water Propulsion System . . . . .	6
7. Schematic of Coanda's Explanation . . . . .	8
8. Normalized Thrust vs. Throat Diameter . . . . .	8
9. Three-Dimensional Coanda Nozzle . . . . .	24
10. Schematic of Angular Measurement on Half Torus	25
11. Toroidal Coordinates . . . . .	28
12. Zero Degree Deflector . . . . .	32
13. Ninety Degree Deflector . . . . .	32
14. Pressure-Rake . . . . .	33
15. Air Storage Tank . . . . .	35
16. Air Compressor . . . . .	35
17. Globe Valve . . . . .	36
18. Air Bearing . . . . .	36
19. Plenum Flange and Force Balance . . . . .	38

Figure	Page
20. Hydraguide Attachment . . . . .	40
21. Separation . . . . .	47
22. Surface Pressure Distribution at $\Theta = 90$ degrees	50
23. Surface Pressure Distribution, $\phi = 0$ to 45 degrees . . . . .	52
24. (Palermo) Pressure Distribution over Cylinder Surface . . . . .	54
25. Velocity Distribution, $\phi = 0^\circ$ . . . . .	57
26. Velocity Distribution, $\phi = 45^\circ$ . . . . .	58
27. Non-Dimensional Velocity Profile . . . . .	59
28. (Palermo) Non-Dimensional Velocity Profile . .	61
29. Tuft at $\Theta = 120^\circ$ . . . . .	63
30. $\Theta = 90^\circ$ , Turn Efficiency ( $\eta$ ) versus Pressure Ratio . . . . .	67
31. $\Theta = 180^\circ$ , Turn Efficiency ( $\eta$ ) versus Pressure Ratio . . . . .	68
32. (Palermo) $\Theta = 90^\circ$ , Turn Efficiency ( $\eta$ ) versus Pressure Ratio . . . . .	70
33. (Palermo) $\Theta = 180^\circ$ , Turn Efficiency ( $\eta$ ) versus Pressure Ratio . . . . .	71

## SYMBOLS

$C_p$	Coefficient of Pressure
$C_{p_s}$	Coefficient of Pressure on Surface
F	Fahrenheit
$F_H$	Pounds Force in Horizontal Direction
$F_T$	Pounds Force in Total Resultant Direction
$F_V$	Pounds Force in Vertical Direction
H	Height, Inches above Surface
h	Height, Manometer Differential in Feet
$h_s$	Height, Manometer Differential in Inches for the Static Pressure Tube
$h_t$	Height, Manometer Differential in Inches for the Total Pressure Tube
I.D.	Internal Diameter
M	Mach Number
O.D.	Outside Diameter
p	Pressure, Pounds per Square Foot
$p_t$	Total Plenum Pressure
$p_{\infty}$	Ambient Pressure
p.s.i.g.	Pounds per Square Inch Gage
rms.	Root Mean Square
STOL	Short Take Off and Landing

$V$	Velocity, Feet per Second
$V_{\theta}^*$	Local Velocity Divided by Local Maximum Velocity
VTOL	Vertical Take-Off and Landing
$\gamma$	Specific Weight, Pounds Force per Cubic Foot
$\theta$	Angular Measurement in Direction of Flow
$\eta$	Turning Efficiency
$\eta_h$	Horizontal Force Turning Efficiency
$\eta_T$	Total Resultant Force Turning Efficiency
$\eta_v$	Vertical Force Turning Efficiency
$\lambda$	Local Height Divided by Local Maximum Height
$\rho$	Density, Slugs per Cubic Foot
$\phi$	Angular Measurement Transverse to Direction of Flow

## ABSTRACT

This study was initiated as an exploratory investigation of a three-dimensional, axially-symmetric, external ejector, "Coanda nozzle." Certain geometrical parameters were made similar to a two-dimensional nozzle, for ease in direct comparison. The configuration of the three-dimensional nozzle was designed to be a half torus. During the study, areas of interest were sought that might be promising for practical application.

A literature review of the Coanda phenomenon was conducted. The review indicated a scarcity of three-dimensional reports. The study was conducted by investigating the nozzle surface pressures, the jet sheet velocities and thickness, and the forces produced by the flow. It was found that no substantial force augmentation was produced. Pronounced surface pressure undulations were recorded. The velocity profiles of the flow did not exhibit any similarity. The flow exhibited properties of separation after 120 degrees of turning. This nozzle configuration offers no apparent advantage over the two-dimensional version.

The test apparatus used does offer an expeditious direct method of obtaining data with minimum calculations.

## CHAPTER I

### INTRODUCTION

#### 1.1 General

Numerous ingenious inventions have resulted from the discovery of a fluid-flow phenomenon called the "Coanda effect" after its discoverer, M. Henri Coanda, a Rumanian engineer, whose first patent dealing with the application of the effect was filed prior to 1935. The Coanda effect may best be understood by reference to Figure 1, as follows: Fluid constrained to two-dimensional flow and discharged from a rectangular or annular slot will be deflected from its initial direction to flow along the flap. In unchoked flow, this deflection results in (a) a pressure reduction in the slot and throughout the interior of the jet, (b) an acceleration of the flow in the region of the corner, and (c) an entrainment of fluid from the surrounding medium by the jet. Further deflection of the stream may be accomplished by the addition of a series of such flaps, the preceding phenomenon being repeated at each corner.

Great interest has been shown in this fluid dynamic phenomenon. Coanda claims the phenomenon to be applicable

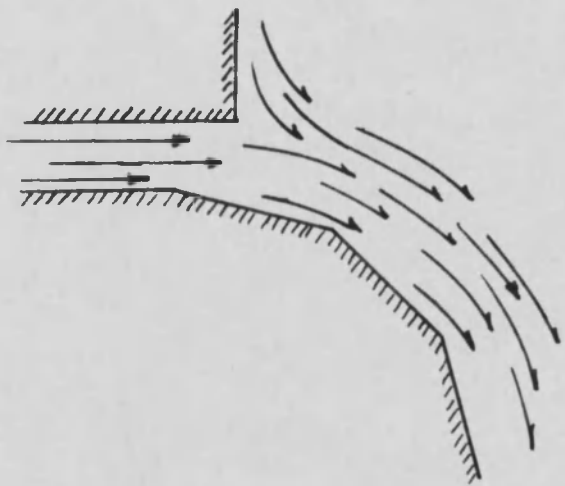


Figure 1. Basic "Coanda Effect" Nozzle

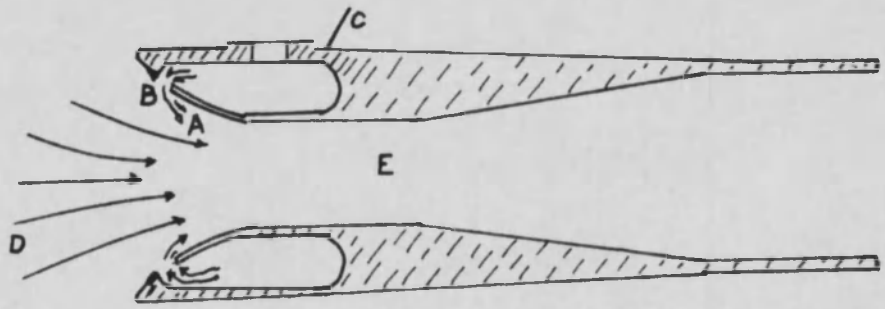


Figure 2. Induced Flow Nozzle

to induced flow (thrust augmentation) units; a high lift, low drag wing; and various types of prime movers. Voedisch (23)\* reported several Coanda device applications.

An induced flow (thrust augmenting) nozzle is shown in Figure 2. In this nozzle, a working fluid A issues from an annular Coanda slot B into a nozzle C, just before the venturi section E. The purpose is to induce a flow D through the nozzle, and produce a flow or thrust augmentation. Initial mixing of a primary and secondary fluid requires large surface contact between the primary and secondary jet. Two methods of ejecting a primary stream into an induced flow nozzle are by using a central jet, found in standard jet pumps, and by a ring jet, found in the Coanda nozzle.

A high-lift, low-drag wing is shown in Figure 3. Air is blown through a Coanda slot A, over the wing B, which has Coanda steps, D, E, F., etc. Many ways have been proposed to increase lift of aircraft wings. Some have attempted to control the boundary layer by either blowing it away or sucking it inside the wing for disposal. The Handley Page wing shown in Figure 4 uses an interconnecting passage between the upper and lower wing surfaces, and only at high angles of attack, does the system operate when air is blown over the upper surface of the wing.

---

\* Numbers in parentheses refer to REFERENCES.

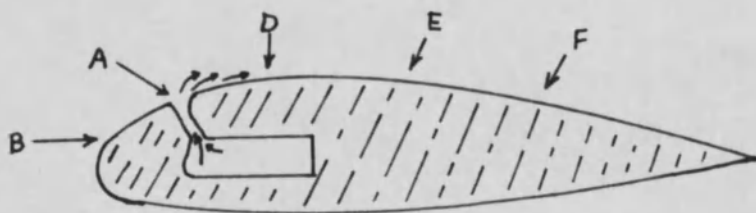


Figure 3. High-Lift, Low-Drag Wing

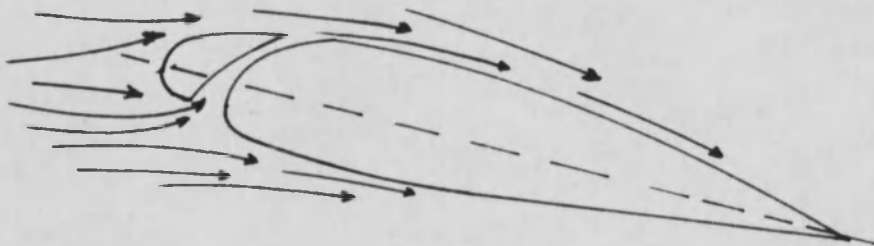


Figure 4. Handley Page Wing

A wind tunnel fan is shown in Figure 5. Air is pumped through Coanda slots A, at each corner of the triangular devices shown, and surrounding air is entrained into a stream which follows around the periphery of the walls. Coanda claimed the speed is augmented at each corner and a very high speed can be attained. The amount of air admitted to the system is recovered at B and recirculated to the Coanda slots A.

A water propulsion system is shown in Figure 6. By using the Coanda device in the nose of a torpedo or ship, and ejecting fluid A through the slot B, the torpedo C will move forward. Reasonable propulsion efficiencies have been obtained with such an arrangement; although not greatly superior to a good propellor, it has the advantage of not being subjected to cavitation troubles at high speeds.

These devices and speculation by Coanda on the use of his "Effect" on wings to control the flow, design of jet engines in which the fluid is ejected from a slot around the nose of the body, and watercraft supported by planing surfaces and propelled by "Coanda Nozzles" have no doubt motivated investigators to explore the basic principles, as well as the practical applications of the Coanda effect. Sproule and Robinson (19) interviewed M. Coanda while he was being detained in Drancy Internment Camp, Paris, France. They deduced that he is more of a professional

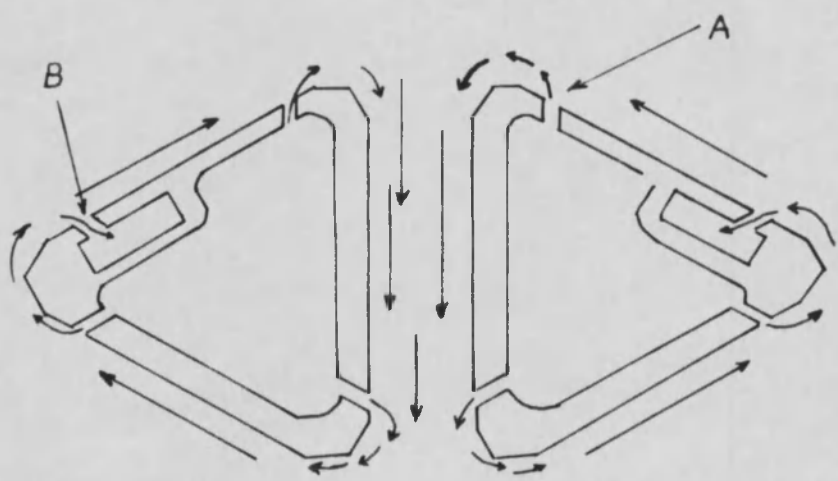


Figure 5. Wind Tunnel Fan.

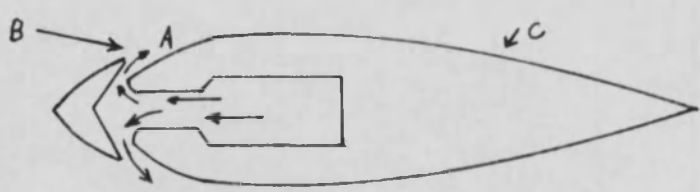


Figure 6. Water Propulsion System

inventor than an engineer. Nevertheless, his theories regarding induced flow are still being investigated for better understanding of the basic mechanisms and higher efficiencies of devices employing the Coanda effect.

## 1.2 Historical Development

When M. Henri Coanda was interrogated in 1944 (19), it was learned that he was a Rumanian engineer who directed a research laboratory at Societe Coanda, 12 Rue Honnet, Clichy, Paris. During the previous decade, Coanda had been developing a theory concerning the kinetic flow of fluids. Coanda expounded upon his theory as the phenomenon which occurs when a stream of fluid is ejected at high speed from a slot fitted with one half of a divergent passage. The stream is deflected from the axis of flow and subsequent turning can be achieved by making several such steps in series. The mass flow and the velocity of the stream are increased. Coanda claimed that it was possible to turn the stream 180 degrees by the proper selection of Coanda deflection plates. He envisioned the flow schematically as shown by Figure 7a. A mass of air is ejected from a slot at a given velocity. If half of a divergent passage is fitted to the slot, as shown in Figure 7b, the stream filaments will follow the slope of this extension and induce further air to join the main stream as shown in Figure 7c. By attaching a second

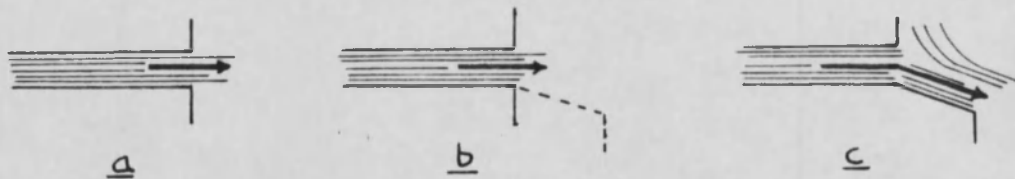


Figure 7. Schematic of Coanda's Explanation

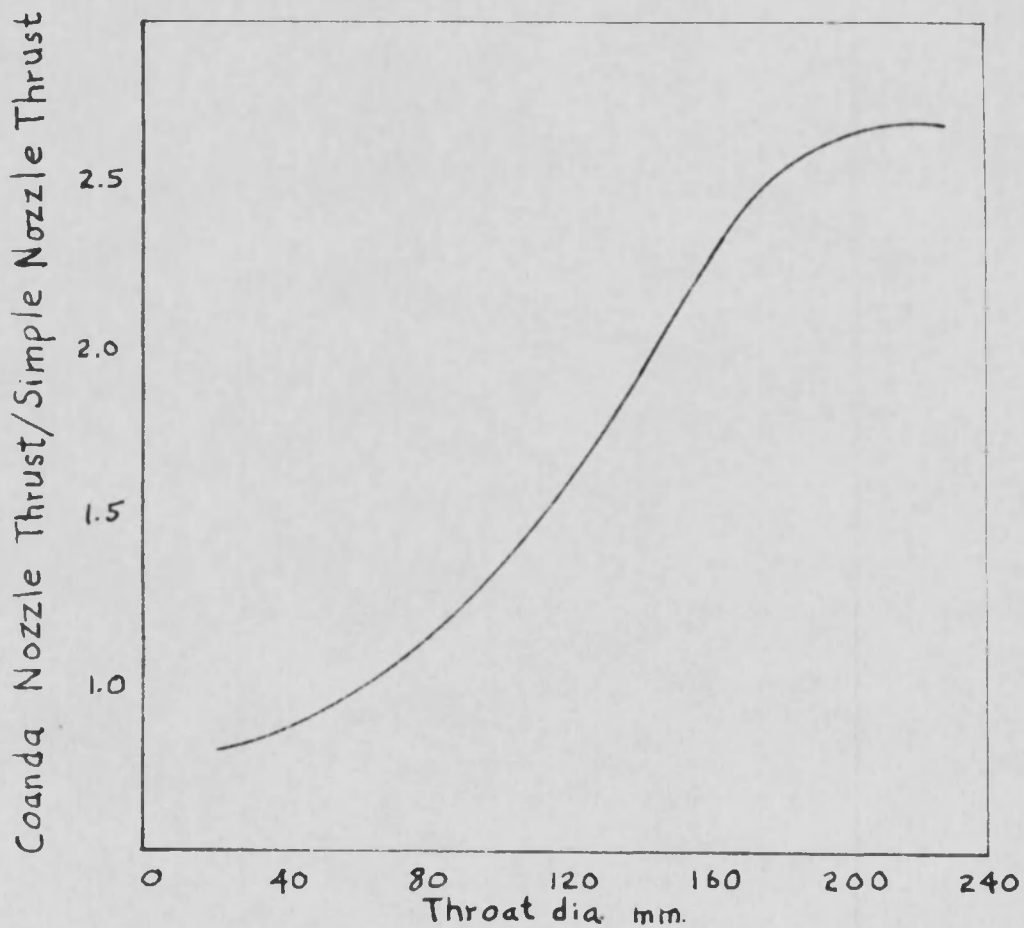


Figure 8. Normalized Thrust vs. Throat Diameter

portion of a divergent passage with the first, the air will again be turned through the angle of this passage and still further air will be induced to flow with the main air stream. Optimum angles of the passages as quoted by Coanda are approximately 31 degrees for the first, 28 degrees for the second, 25 degrees for the third, etc., decreasing by about 3 degrees per stage.

Coanda's experiments in the early stages attempted to apply this principle to the design of exhaust systems for reciprocating engines in order to improve the scavenging characteristics. Later in 1942, Coanda obtained a contract from the Germans for the development of a propulsion system for snow sleds, supposedly for use in Russia. This particular application gave greater emphasis to research on thrust augmentors. Apparently, the Germans were not convinced of its utility or else more pressing matters were at stake because they stopped the work after several nozzles varying in throat size from 20 mm. to 100 mm. were built and tested. Coanda claims to have completed sufficient tests to prove the worth of the scheme. Coanda normalized the thrust obtainable from a "Coanda Nozzle" to that obtained from a simple nozzle utilizing the same mass flow and at the same pressure of the primary fluid in both nozzles. The normalized thrust versus throat diameter is shown in Figure 8. By this

research, Coanda did establish some of the parameters for this type of nozzle flow. He found that for a given set of conditions there was an optimum throat diameter and optimum slot size for every size throat and pressure ratio.

At the time, 1944, of the interrogation of Coanda, the Usines Chasson motor car radiator manufacturers in Asnieres, Paris, were using the Coanda effect in a practical application. The firm reported that they had studied the problem and constructed a 150 mm. nozzle fitted with a 0.10 mm. slot and using air as a working fluid at a pressure ratio of 1:1.5 induced a flow of 20 times that of the working fluid (19).

From this comparatively recent historical beginning with Coanda's myriad of innovations, numerous attempts have been made to combine proper parameters for a "breakthrough" that would produce a substantial thrust augmentation, as well as turning efficiency.

### 1.3 Chronological Review of Literature

A large number of references (50 or more) are now available on the Coanda effect and its various aspects. It will be noted that the preponderance of work has been done on two-dimensional flow. In general, the earlier attempts to understand the Coanda effect could hardly be

classified as an analytical approach but more of an empirical approach. The results of the many empirical observations have provided the broad guidelines of interest for analytical investigation. Noticeably lacking in the review of literature is the analytical investigation of the three-dimensional Coanda effect.

Gates (6) reports that the earliest recorded interest in the tendency of a flow to cling to a surface is the work of M. Lafay in 1918 on the Chilowsky effect. M. Lafay's interpretation of the Chilowsky effect was, "decreasing the resistance opposed by the air to a projectile by providing it in front with a sort of beak which emits transversely, through a circular orifice, a sheet of fire." M. Lafay modified this arrangement by reducing the length of the beak to zero. This enabled M. Lafay to reduce by 50 per cent the initial drag. However, no indication is given of the energy expended in producing this substantial decrease of drag on the projectile.

Schubauer (18) applied the Coanda effect to an external ejector placed in the nose of a dirigible. When compared with a nozzle in the tail of the dirigible, he recorded a thrust loss.

During this period, M. Henri Coanda proposed to use the phenomenon in a variety of devices (6). Coanda observed that when air was ejected from a rectangular

slot, it would attach to an inclined surface fixed to the nozzle exit. Because he found a maximum angle for the inclined surface (about 30 degrees), he was able to deflect the flow through 180 degrees by placing a series of flat plates, each at an angle to the preceding one. There is an increase in the velocity and mass flow of the fluid, and the fluid tends to follow around the surfaces while entraining adjacent free air. The jet tends to break away at the intersection of the surfaces, and this causes a pressure drop that pulls the jet back toward the surface. This caused Coanda to emphasize the need for a sharp intersection between the nozzle and the attached deflection surface. Coanda concluded that the increase in mass flow through the nozzle must produce an increase in the available jet thrust.

Coanda flow was first analyzed by Metral (13). He used a technique of conformal mapping and was successful in showing that the air jet flow along a single sharp-edged bend increases the mass flow rate. This result was verified by an experiment on automobile and motorcycle engines equipped with Coanda nozzles.

Sproule and Robinson (19) made a detailed report on the interrogation of Coanda and obtained models and data from him. The data showed augmentation ratios as high as

2.7 for an internal ejector. They obtained sketches depicting several ideas for annular external ejectors.

Voedisch (23) made an analytical investigation of the Coanda effect. He also traced the history of Coanda's efforts to use the phenomenon for various devices. Voedisch's analysis verified Coanda's findings, that an increased mass rate of flow issued from a nozzle and flowed along an inclined wall. Voedisch also showed that the stationary ambient air is entrained along the primary jet.

Boyer (2) and Marwood (12) made an experimental evaluation of the external ejector using a single flat deflection surface. They studied the reduction of the pressure in the nozzle exit and increase of mass flow of the jet. Relationships of various parameters such as nozzle overhang, pressure ratio, width of jet, and deflection angle were determined. Their test results verified that two-dimensional Coanda flow clings to the surface.

von Karman (26) made a theoretical analysis in an attempt to explain the superior performance claimed by Coanda for his internal ejector. von Karman predicts a superior augmentation for ejectors when the primary fluid is injected along the wall of the tube rather than from a centrally-located nozzle. He believes that this is most likely to be the reason for the good entrainment

characteristics of annular internal jet ejectors. A greater lack of uniformity of fluid velocity will occur at the beginning of the mixing region when the primary jet is injected along a wall. This lack of uniformity of fluid velocity where mixing starts is an element that increases ejector thrust augmentation.

Yen (27) made another theoretical analysis in which he replaced the angled flat plate by a smoothly curved surface. He concluded that 1) viscous effects are predominant and an inviscid analysis is not very meaningful, 2) replacing the sharp corner by a smooth transition caused a reduction in the increase of mass flow through the nozzle over the sharp corner case.

von Glahn (24 and 25) investigated the performance of a series of single-flat-plate, multiple-flat-plate, and some curved deflection surfaces over a wide range of operating pressures in conjunction with rectangular convergent nozzles. The vertical and horizontal forces and pressure distributions along the deflection surfaces were measured. He was able to achieve turning efficiencies of 88 per cent for multiple flat plates and 81.5 per cent for the curved deflection surface. His pressure distributions over the curved surfaces were characterized by large fluctuations in the suction pressure. These fluctuations he believed to be caused by local discontinuities in the

surface contour. To keep the flow attached to the deflection surface, he found it necessary to have side plates extending over the whole length of the deflection surface. He reasoned that the detachment point is located where the local surface pressure approaches the ambient pressure.

Gates (6) of Hiller Aircraft Corporation tested both the two- and three-dimensional Coanda nozzle, external ejector, in the search for substantial thrust augmentation. He defined thrust augmentation as the ratio of the measured vertical force to the measured undeflected thrust of the basic nozzle. Gates used the same deflection surface defined by a cubic equation developed by Cornell Aeronautical Laboratory where augmentation ratios of 1.7 to 1 were obtained. But Gates was unable to obtain any thrust augmentation. It is believed that the discrepancy lies in a misunderstanding of the measured undeflected thrust of the basic nozzle (1). Gates did conclude the following:

- 1) Turning efficiency is high.
- 2) Ground effect was tested by placing orthogonally a five-foot square piece of 3/4 inch plywood near the end of the model surface. With two-dimensional Coanda nozzle, ground effect has negligible effect on the vertical lift,

but ground effect increases the horizontal thrust by a factor of three.

- 3) Entrainment of ambient fluid is not vigorous and its direction is normal to the primary jet.
- 4) No static thrust augmentation can be obtained by an external ejector.

In the particular three-dimensional configuration employed by Gates, he found insignificant difference in maximum performance between the two-dimensional case and the three-dimensional case. Neither case gave any thrust augmentation. The primary difference in the characteristics of the two different models occurred in the breakaway from the surface by increasing the supply pressure in the tested flow regime for the three-dimensional case. Gates reports that the breakaway phenomenon requires additional study for proper and complete understanding.

Coanda (5) used an internal ejector nozzle and found thrust augmentation (measured thrust compared with theoretical thrust) of 1.32 and 1.46 for pressure ratios of 1.5 and 0.3. (Feeding pressure minus atmospheric pressure divided by atmospheric pressure), respectively. He used the surface pressure measurement to conclude that the "lip" of his nozzle produced most of the thrust and the divergent section produced a drag working in the opposite direction. Coanda stated, "If we consider the

very encouraging results obtained, it appears that it would be quite important to ascertain the real theory of such nozzles. But, this will need an important study which would require a special team well trained in aerodynamic and this during a fairly long time."

Bourque and Newman (3) made a study of the reattachment of a two-dimensional, incompressible, turbulent jet to an adjacent, inclined, flat plate. At the slot lips, the jet separates from the boundaries and reattaches to the plate downstream. This phenomenon is associated with the lowering of the pressure between the jet and the plate with the entrainment of fluid there. The flow becomes independent of both the length of the plate and the Reynolds number when these parameters are sufficiently large. The flow, scaled with respect to the width of the slot, is then uniquely determined by the plate inclination.

Sterne (21) used a special nozzle with a boosting device, both manufactured by SFERI-Coanda in an attempt to obtain higher thrust augmentation. For purpose of analysis, a reference thrust " $F_0$ " is defined as the force which would be produced if the pressure of the primary air were reduced isentropically to atmospheric pressure, and the resulting air velocity directed in a rearward axial direction. An amplification factor "A" is defined as the

ratio of "F", the total thrust under any condition, to "F<sub>0</sub>". Sterne obtained a thrust amplification of 1.34 without the boosting device and 1.56 with it.

Bailey (1) used a deflection surface that was not rigidly attached to the nozzle. This technique of mounting the deflection surface permits more flexibility in testing various surfaces and a more sensitive force balance. He proposed a parameter of surface radius compared with nozzle height for correlating data. A vertical turning efficiency of 92 per cent was the maximum obtained with a smooth curved surface at a pressure ratio of 2 to 1. The surface pressure distributions are characterized by a region of separated flow and regions of decreasing and increasing pressure on the curved surface. He concluded that a decrease in turning efficiency could be expected at high flow speeds, due to the increased total pressure loss through shock wave systems.

Roderick (17) continued the work of Bailey but used three different two-dimensional convergent-divergent nozzles, instead of simple convergent nozzles. He sought to determine how supersonic and under-expanded jets of various thicknesses behave in connection with smoothly-curved Coanda deflection surfaces. The vertical and horizontal forces acting on such surfaces were measured and pressure distributions were recorded. His results showed

that turning of two-dimensional supersonic and under-expanded jet sheets by a smoothly curved deflection surface can be easily accomplished:

- 1) There is an optimum initial angle for the vertical turning efficiency, and both increase with nozzle pressure ratio; but the horizontal turning decreases.
- 2) Thicker jets turn less efficiently.

Korbacher (9) reported high turning efficiencies for detached deflection surfaces, i.e., in the ventilated clinging flow regime. He did not use a configuration conducive to thrust augmentation. The sharp leading edge of the deflection surface tends to reduce the secondary flow that can be induced. With a jet thickness of one-eighth inch, it was possible to cause the horizontally ejected jet to jump horizontal and vertical gaps of more than 8 and up to 4 times the jet sheet thickness, respectively. He obtained high turning efficiencies (96 per cent for 90 degree deflection). He offers a theory to predict and correlate the deflection surface pressure, as related to the radius of the deflection surface and thrust of the primary jet.

Levin and Manion (10) analyzed the attachment of a submerged, incompressible, two-dimensional, turbulent jet to an adjacent straight wall. Parametric equations were

developed that predict the point at which the jet attaches as a function of wall angle and offset distance. These equations should be helpful in designing elements based on the Coanda effect because they provide an analytical method, independent of the particular fluid.

Gates (7) found that thrust augmentation was definitely possible by the ventilated clinging flow deflection principle. With one of his configurations at optimum ventilation there was produced a thrust augmentation of 6 per cent, based on the primary jet thrust, while deflecting the jet 58 degrees from its original direction. Gates states, "This can be compared to a loss of about 10% for an optimum Coanda effect deflection system." Side plates were required for best performance of the configuration tested, but caused a thrust loss of about 2 per cent due to side plate frictional effects. On the basis of a thick jet analysis, Gates suggests that the tested configuration may not be the optimum for thrust augmentation.

Chang (4) made a survey of 31 references on Coanda flow to provide better understanding of the mechanics of the flow and its practical use of fluid amplification. Excerpts from the references and a discussion of them are cleverly arranged so that the Coanda effect is defined. Then the references are used to discuss Coanda flow:

Inviscid Incompressible, Viscous Incompressible, Compressible, Practical Application, and Future Development. Chang concludes, "The solution of viscous Coanda flow will contribute greatly, accompanied by experience, to further development of mechanics of fluid amplification."

Triner (22) studied two-dimensional Coanda flow by investigating the flow over a cylinder produced by a slot tangential to the surface. Pressure ratios of about 1.0 to 1.5 were used and flow attachment remained high. Turning efficiency of 97 per cent (the ratio of measured lift to measured axial thrust) was obtained for 90 degrees of turn.

Palermo (16) extended the work of Triner (22) by obtaining experimental data that he was able to reduce to a more analytical basis. A turning efficiency of approximately 100 per cent was obtained for 90 degrees of turn. The velocity profile was measured at Mach .18 and non-dimensionalized. A Pohlhausen velocity profile was determined for the experimental non-dimensional profile. Surface pressures were measured over a range of pressure ratios of 1.02 to 2.50 and no separation on the cylinder was reported.

This wealth of literature shows many facets of the Coanda flow phenomenon. The parameters of the flow found in the literature should provide an insight for modifica-

tion of a deflection surface configuration to obtain optimum performance. But, a suitable configuration for practical application needs to be found that will offer an improvement over existing devices.

#### 1.4 Purpose of the Study

The objective of this study is to conduct an exploratory investigation of a three-dimensional deflection surface with an annular type slot issuing a jet at various pressure ratios. The three-dimensional Coanda nozzle will have geometric parameters similar to a two-dimensional nozzle by Palermo (16) for direct comparison of results. This will be accomplished by:

- 1) Analyzing the surface pressures at various pressure ratios.
- 2) Exploring the velocity profile and jet thickness for assumed incompressible flow.
- 3) Measuring the horizontal and vertical forces produced by the Coanda flow.

## CHAPTER II

### THEORETICAL CONSIDERATIONS

#### 2.1 General

The three-dimensional model used had a surface profile of the same magnitude as the cylinder studied by Palermo (16). The configuration of the three-dimensional model can be described as a half torus with base plate and annulus, Figures 9 and 10. The nozzle aspect ratio for the half torus was 62.5 and for the cylinder was 39.8, slot circumferential length divided by slot height. The nozzle aspect ratio of the half torus was 1.57 times larger than the nozzle aspect ratio of the cylinder. It was theorized that this greater aspect ratio would result in a thinner primary jet sheet. The increase in area ratio of mixing surface to jet exit area would cause an increase in performance by providing a better opportunity for the entrainment of secondary air.

Also, the flow from the torus slot gains an additional degree of freedom by expansion of the primary jet in an angular direction about the longitudinal axis of the nozzle. The additional degree of freedom is transverse to the angular flow about the circumferential axis



Figure 9. Three-Dimensional Coanda Nozzle

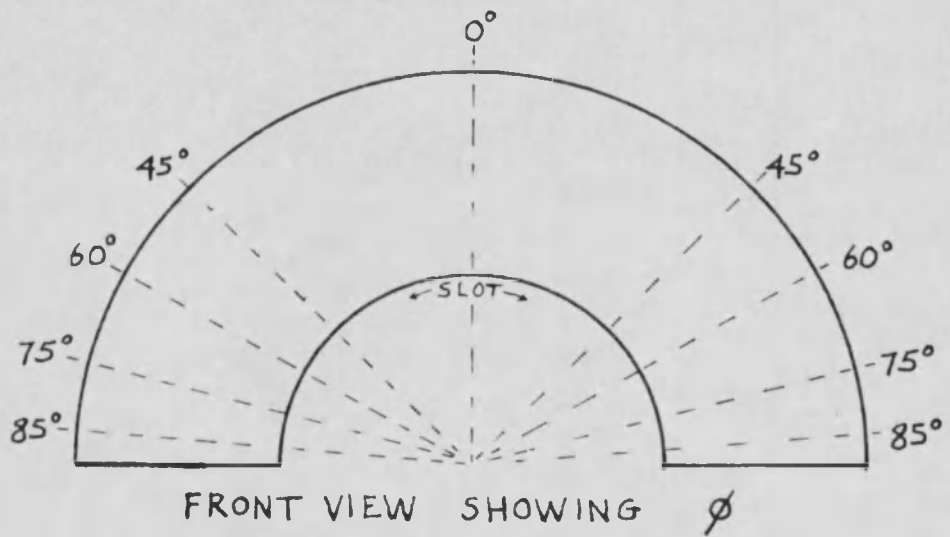
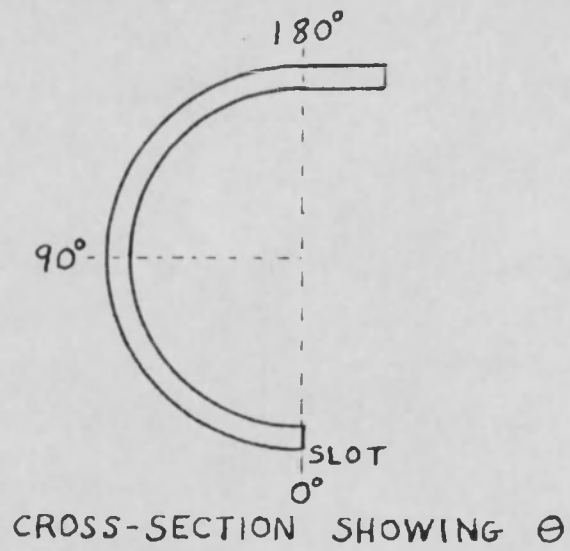


Figure 10. Schematic of Angular Measurement on Half Torus

of the torus. A lower internal jet pressure and greater entrainment of secondary air with improved performance compared with the two-dimensional flow over the cylinder was anticipated. The above speculation was prompted by the awareness of the existing theory of two-dimensional flow.

## 2.2 Three-Dimensional Flow

The half torus configuration was deliberately chosen instead of a complete torus. It was believed that three-dimensional axially-symmetric annular flow around a complete torus would tend to cancel vertical and lateral forces. Due to the symmetry of a complete torus, one would expect only horizontal, thrust, forces to be produced.

With the half torus configuration, part of the symmetry has been removed; namely, the symmetrical half that could be the portion of the torus capable of cancelling the vertical forces on the remaining half. Theoretically, it appeared that if both a vertical and horizontal force could be measured, then additional data would be available for solving equations to describe the flow.

A review of the literature revealed that most investigators either did not attempt to explain the equations describing the three-dimensional aspects of Coanda flow, or made assumptions that were not justified for this particular half torus configuration. Pai (15) discussed

the three-dimensional subsonic flow of a jet of inviscid fluid and stated,

"It is difficult to develop a mathematical theory of three-dimensional flow of a jet in general, because we do not have such a powerful method similar to theory of complex variables in the two-dimensional case. Little progress has been made for the three-dimensional problem. However, if the flow in the jet is essentially parallel to its axis, a small perturbation method may be used to explain some of the phenomena in the jet."

Sridhar (20) states that it has been shown that an axially-symmetric case can be solved directly from the two-dimensional solution with the help of appropriate transformations.

To facilitate the formulation of the equations describing the Coanda flow over the half torus, it was decided to choose a suitable coordinate system and use the Navier-Stokes equations of motion. Hughes and Gaylord (8) have published the Navier-Stokes equation in generalized orthogonal curvilinear coordinates. The most appropriate coordinate system for this particular configuration and its associated flow appeared to be one of the variations of orthogonal curvilinear coordinates, the toroidal coordinate system. Figure 11 is a sketch of a toroidal coordinate system. Moon and Spencer (14) described the toroidal coordinate system and presented the transformation equations relating toroidal and cartesian coordinates in conjunction with the sketch and symbols of Figure 11.

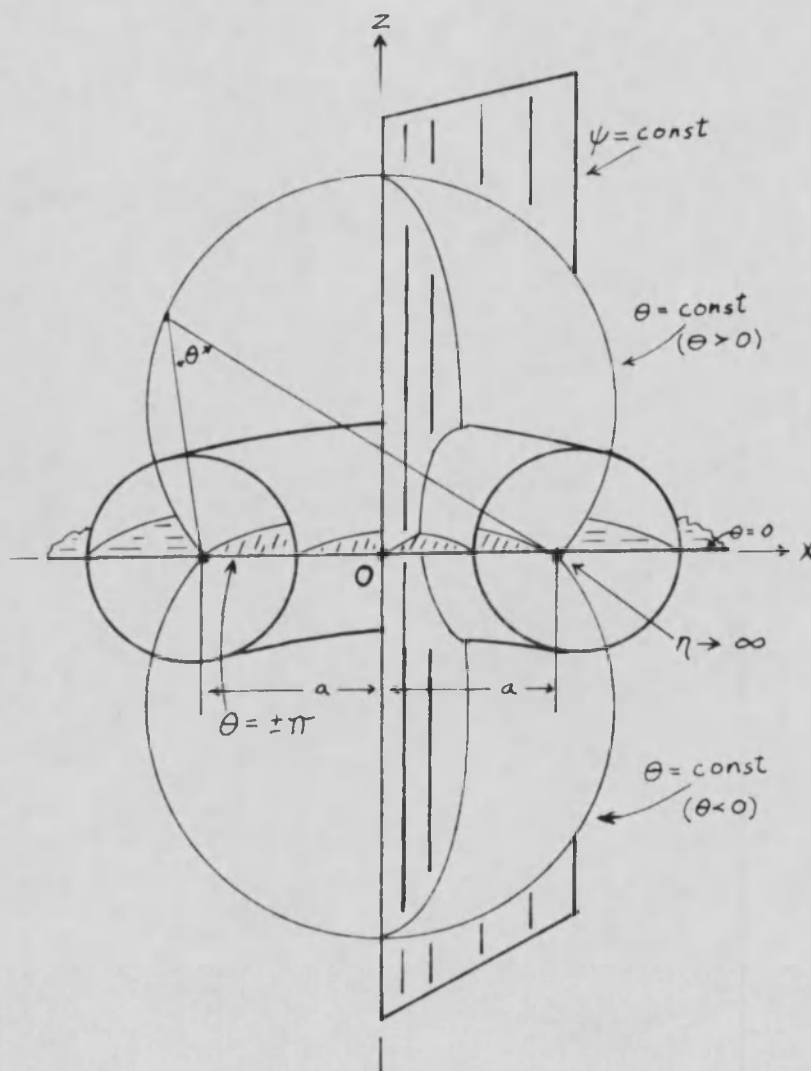


Figure 11. Toroidal Coordinates

$$X = \frac{a \sinh \eta \cos \psi}{\cosh \eta - \cos \theta}$$

$$Y = \frac{a \sinh \eta \sin \psi}{\cosh \eta - \cos \theta}$$

$$Z = \frac{a \sin \theta}{\cosh \eta - \cos \theta}$$

The metric coefficients for toroidal coordinates are:

$$g_{11} = g_{22} = \frac{a^2}{(\cosh \eta - \cos \theta)^2}$$

$$g_{33} = \frac{a^2 \sinh^2 \eta}{(\cosh \eta - \cos \theta)^2}.$$

Toroidal coordinates are generated by rotating circles about the Z-axis. The surfaces of constant  $\eta$  are toroids, the surfaces of constant  $\theta$  are spherical bowls, while the surfaces of  $\psi$  equal to a constant are half planes through the axis of symmetry. This axis is called the Z-axis in three-dimensional space. Points above the xy-plane are distinguished from points below this plane by employing positive  $\theta$  for the former and negative  $\theta$  for the latter. Thus  $\theta$  varies from  $-\pi$  to  $+\pi$ , while  $\eta$  varies from 0 to  $+\infty$ .

By using the toroidal coordinate system, the approach to the problem of formulating the equations describing the flow over the half torus was established.

In principle, the Navier-Stokes equations would be restated in terms of toroidal coordinates by using the appropriate transformations. The transformed equations would be non-dimensionalized and an order of magnitude analysis performed. The order of magnitude analysis would permit discarding the insignificant terms of the equations. The equations could then be presented in their simplest form.

Since the nature of this study is an exploratory experimental investigation, the preceding outline of a theoretical analysis will be reserved until a later section pertaining to data analysis. In the data analysis section, it will be determined if the Coanda flow is well-behaved and exhibits similarity of the velocity profiles. If this condition exists, then the theoretical analysis will be continued, and should prove fruitful for solving the equations describing the Coanda flow over the half torus.

## CHAPTER III

### TEST APPARATUS AND DATA MEASURING EQUIPMENT

#### 3.1 Test Apparatus

The test apparatus consisted of two air sources, air inlet pipes, a throttling valve, two air bearings, a plenum chamber, a force balance, static and total pressure rakes and a Coanda nozzle. Components of the test apparatus were constructed in the Mechanical Arts Building and assembled in the Aerospace Laboratory at The University of Arizona. The nozzle was machined from aluminum stock and incorporated surface pressure ports. The inherent turning capability of the nozzle was 180 degrees. Deflectors were made in order to limit the flow to 0 degrees and 90 degrees, Figures 12 and 13. Pressure rakes could be placed in the Coanda flow at any position by using a piece of soft copper tubing as a stinger, Figure 14. The force balance was used to separate the vertical and horizontal forces. Components of the test apparatus were mounted on a test stand with adjustable legs to insure a level platform for the conduct of the experiment.



Figure 12. Zero Degree Deflector



Figure 13. Ninety Degree Deflector

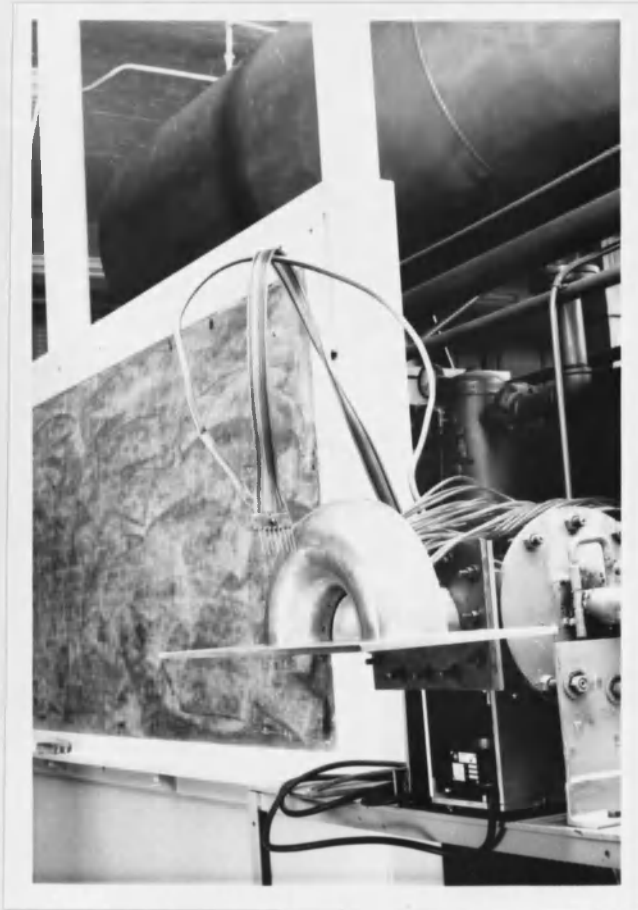


Figure 14. Pressure Rake

### 3.1.1 Air Supply

The primary air supply was a storage tank with a capacity of 220 cubic feet, Figure 15. A Gardner-Denver compressor, Figure 16, capable of displacing 142 cubic feet of air per minute supplied the storage tank and generated 120 p.s.i.g. in the tank. A two-inch globe valve was placed in the air line between the storage tank and the plenum for control of plenum pressure, Figure 17. Two pipes (1-3/8 inches I.D.) on opposite sides of the plenum served as inlets of air through the air bearing to the plenum chamber, Figure 18.

A second air source for the air bearings was obtained from a common air supply piped throughout the laboratory.

### 3.1.2 Air Bearings

Freedom of travel in the vertical and horizontal directions was provided for the plenum by air bearings. The air bearings operated on the principle of a cushion of air between two flat bearing surfaces. One surface was attached to the plenum and the other surface attached to the air inlet pipe. The air inlet bearing surfaces on opposite sides of the plenum were connected by tie rods. The tie rods were adjustable so that a clearance of 0.004 inch existed between bearing surfaces. An independent air source from the main air supply for

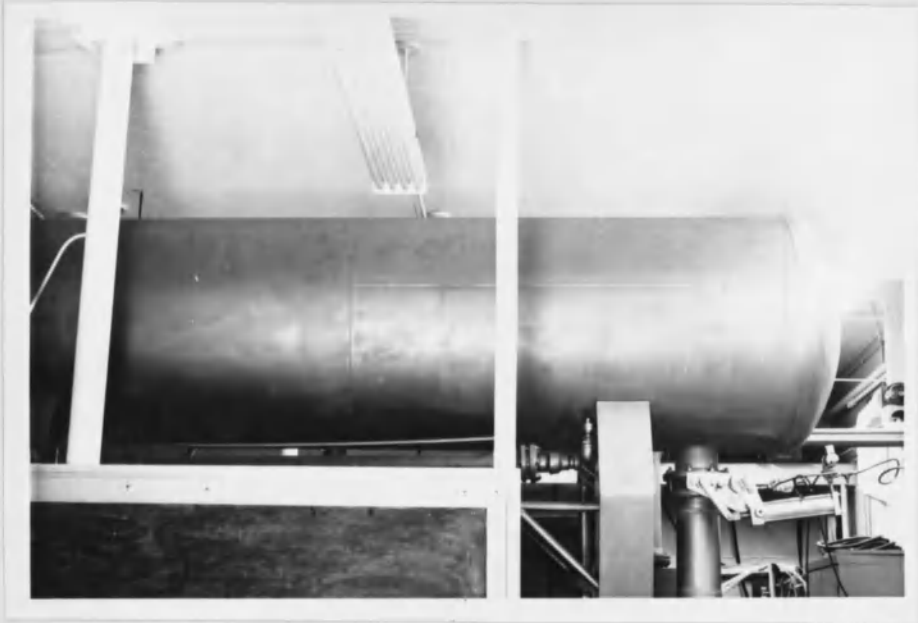


Figure 15. Air Storage Tank



Figure 16. Air Compressor



Figure 17. Globe Valve

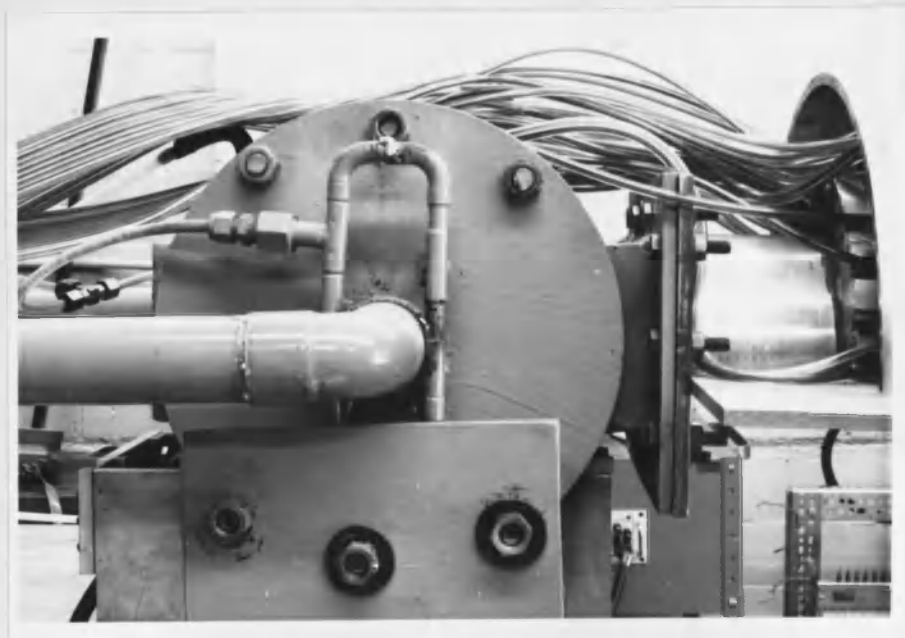


Figure 18. Air Bearing

the nozzle was regulated to 10 p.s.i.g. To prevent corrosion on the steel bearing surfaces, a light lubricant was applied. Triner (22) reports that air bearings eliminated lateral loads on the plenum chamber.

### 3.1.3 Plenum Chamber

A plenum chamber was designed to operate at 150 p.s.i.g. Pieces from a 5/16 inch steel plate were cut, chamfered, and electrically welded together to form a chamber measuring 11 x 7 x 4 inches. Additional strength and rigidity was obtained by passing a 5/8 inch bolt through the top and bottom of the plenum with a 1-inch diameter pipe section acting as a spacer. Air entered the plenum through air bearings from opposite sides. The front end of the plenum consisted of a flange with a 6-1/4 x 3-3/8 inch opening, Figure 19. By using a rubber gasket, it was possible to change nozzles on the common plenum with force balance attached and no perceptible air leak at the new flange connection.

### 3.1.4 Three-Dimensional Coanda Nozzle

An aluminum block measuring 14 x 9 x 3 inches was formed by laminating one inch sheet aluminum stock. Three pieces of one inch thickness were cut to dimensions and laminated together by machine screws and

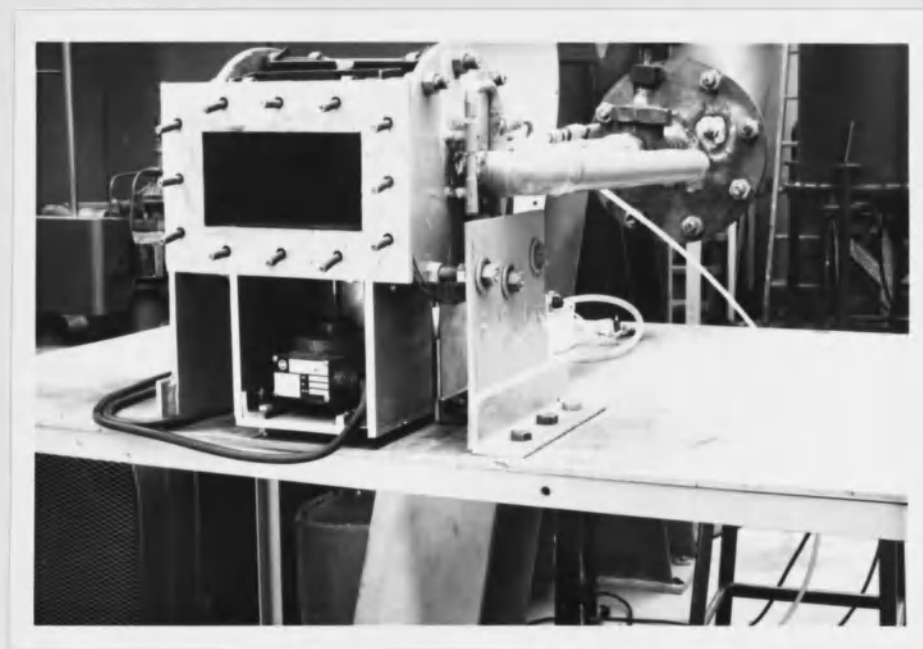


Figure 19. Plenum Flange and Force Balance

Epoxy glue. The block was heated at 140 degrees F. for four hours to strengthen the glued sheets.

A template of the surface profile for the Coanda nozzle was cut from a 5/16 inch aluminum plate. The laminated aluminum block with a piece of 6 inch circular aluminum stock attached was chucked in a lathe. The lathe was equipped with a hydraguide attachment which followed a template and formed the half torus to be used as the deflection surface of the Coanda nozzle, Figure 20.

The radius of curvature for a cross section of the half torus was 2-1/4 inches. This curvature was chosen for ease of comparison with the cylinder of Palermo (16). Surface pressure ports of 1/32 inch diameter were drilled normal to the surface. The pressure ports were spaced at 5 degree intervals near the nozzle exit, 90 degree, and 180 degree positions. The location of a pressure port was given by considering the nozzle exit as 0 degrees and increasing as the flow travels around the deflection surface completing 180 degrees of turn. The rotation of a radial line pivoted on the circumferential axis of the torus was designated as  $\theta$ , with  $\theta$  equal to 0 degrees at the slot, and  $\theta$  equal to 180 degrees when diametrically opposite to the slot. Lateral positions were denoted by considering the symmetrical position on the surface as 0 degrees and increasing to  $\pm 90$  degrees at the

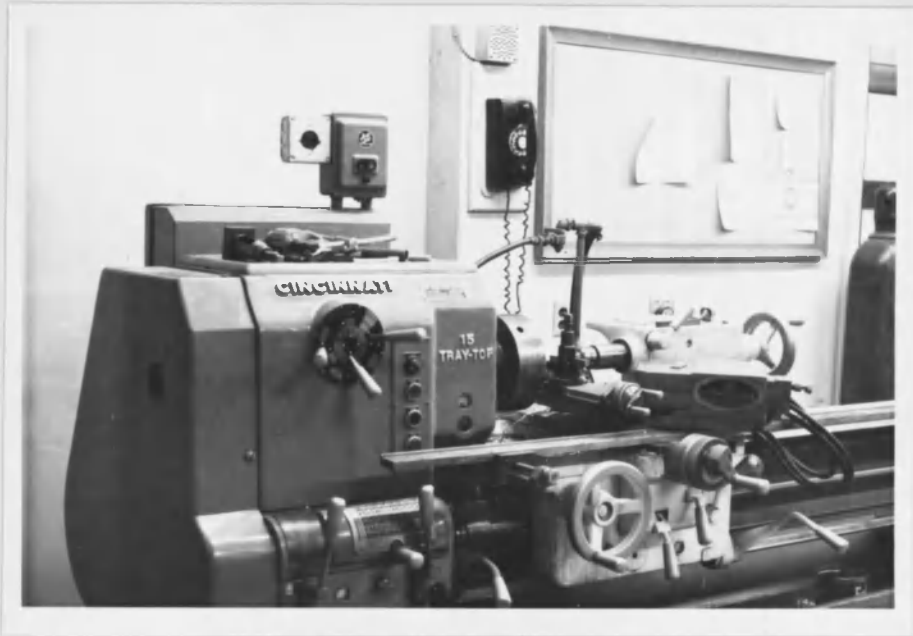


Figure 20. Hydraguide Attachment

base plate. This angular measurement was referred to as  $\theta$  degrees, Figure 10. The pressure ports were staggered in  $\theta$  and  $\phi$  directions with at least 1/4 inch spacing to avoid any disturbance created by a wake around the port.

A nominal slot of 1/8 inch was formed by centering a half hemisphere of aluminum (radius of curvature 2-1/8 inches) inside the half torus. The half hemisphere, half torus, and a mating piece of 5/16 inch steel for the plenum flange were all joined to a 5/16 inch aluminum plate (9 x 20 inches). This base plate is analogous to the side plates used in two-dimensional Coanda flow and completed the composite Coanda nozzle. The deflection surface was checked for roughness with a Profilometer and found to have a surface roughness of 5 microinches rms., indicating a superfinish classification. This finish was obtained by polishing and waxing.

### 3.1.5 Throttling Valve

A 2 inch globe valve rated at 150 p.s.i.g. was placed in the main air inlet pipe, Figure 17. The valve was manually controlled by monitoring the plenum pressure.

### 3.2 Data Measuring Equipment

To explore the Coanda flow associated with this type of Coanda nozzle, equipment was used to measure

surface pressures, static and total pressures in the Coanda sheet, and horizontal and vertical forces produced by the Coanda flow. In addition, tufts were made from fluffy cotton string to provide a visual presentation of the flow direction.

### 3.2.1 Manometers

The mercury manometer used was manufactured by the Aerolab Supply Company, Hyattsville, Maryland. Sixty inches of mercury on each of the twenty tubes could be measured. For lower pressures where greater sensitivity was required, a water manometer of twenty tubes was available. Both the mercury and the water manometer were equipped with an electrical solenoid device that would preserve the pressure readings of the tubes when the solenoid was engaged.

### 3.2.2 Surface Pressure Measurement

The design of the Coanda nozzle facilitated the measurement of surface pressures. Surface pressure ports (1/32 inch diameter) were drilled normal to the deflection surface of the nozzle. On the opposite surface, the pressure ports were counterbored a sufficient depth to insert polystyrene pressure tubing. The tubing was inserted and glued to make an air-tight seal. The other

end was connected to a manometer for direct pressure readings of the individual surface ports.

### 3.2.3 Total and Static Pressure Measurement in The Coanda Sheet

Individual rakes were constructed for measurement of total pressure and static pressure within the guidelines set forth by Liepmann and Roshko (11). For the total rake, brass tubing (I.D. 0.020 and O.D. 0.040) was used. Eight tubes were mounted parallel to each other at 1/4 inch intervals on a steel plate base, thus forming a rake, Figure 14. In order to make a measurement, the rake was attached to a "stinger" (a 3 foot length of soft copper tubing). The rake was then positioned on the Coanda surface so that the alignment of the orifices was normal to the surface with the bottom tube tangential to the surface. This permitted total pressures to be measured at 1/4 inch intervals for 1-3/4 inches into the Coanda sheet with the aid of manometers.

Similarly, a rake was constructed for static pressure measurements. Brass tubing (I.D. 0.015 inches and O.D. 0.030 inches) was used. The static orifice was drilled 1/2 inch from the blunted end of the tube. The orifice on the bottom tube of the rake was placed tangentially to the surface and static pressures measured by the same technique used for total pressure measurements.

### 3.2.4 Total Pressure Measurement in the Plenum Chamber

Two methods were used to measure the plenum pressure. The most direct method was by attaching a pressure tube from the plenum to a water or mercury manometer. This method was also used to measure surface pressures or total and static pressures in the Coanda sheet. The other method depended upon a temperature compensated pressure transducer manufactured by Statham Instruments, Inc., Los Angeles 64, California. The pressure transducer was calibrated over its range of measurement against a mercury manometer for use in conjunction with a Leeds and Northrop Potentiometer or the Y direction of a Moseley Autograf, X-Y Recorder. Calibration graphs were prepared that enabled readings on the two electrical recording instruments to be interpreted as pressures. This method was used for determining plenum pressures during the force measuring experiments.

### 3.2.5 Horizontal and Vertical Force Measurement

A resultant force was produced by the flow of air through the Coanda slot. This force varied depending upon the configuration of the nozzle and the plenum pressure. The resultant force was transmitted from the Coanda nozzle to the plenum and then to the force balance through rigid connections. The force balance was designed

to resolve the resultant force into horizontal and vertical forces, Figure 19. Detailed plans used for construction of the force balance are available at Aerospace Laboratory, The University of Arizona. A basic assumption used for the force balance was that a negligible force was required to deflect spring steel shim stock laterally a minute distance, but that this deflection was sufficient to produce an effect on sensitive load cells. This assumption was verified by calibration with dead weights. A linear curve was plotted for pounds versus electrical readings on the Leeds and Northrop Potentiometer, and the X direction of the X-Y Recorder. The nomenclature of the load cells used was SR-4 Load Cell, Type U-1, capacity 500 pounds for the horizontal direction and SR-4 Load Cell, Type U-1-B, capacity 50 pounds for the vertical direction. Both load cells were manufactured by Baldwin-Lima-Hamilton Corp., Waltham, Mass. In order to standardize the calibration data, a known resistance was applied to a leg of the Wheatstone Bridge incorporated in the electrical recording device circuitry. These data were plotted on the linear curve, and provided a means to standardize the calibration curves for successive experiments. When the electrical recording devices used in the force measurements are available, they offer a rapid and sensitive means of resolving

forces without detailed calculations that have plagued many of the earlier investigators.

### 3.2.6 Flow Visualization

Loosely woven cotton string was cut into  $3/4$  inch sections and unraveled. The sections were taped directly to the surface of the nozzle and observed for their degree of clinging to the surface when subjected to the flow. Figure 21 shows an example and an artificially exaggerated example of the separation.

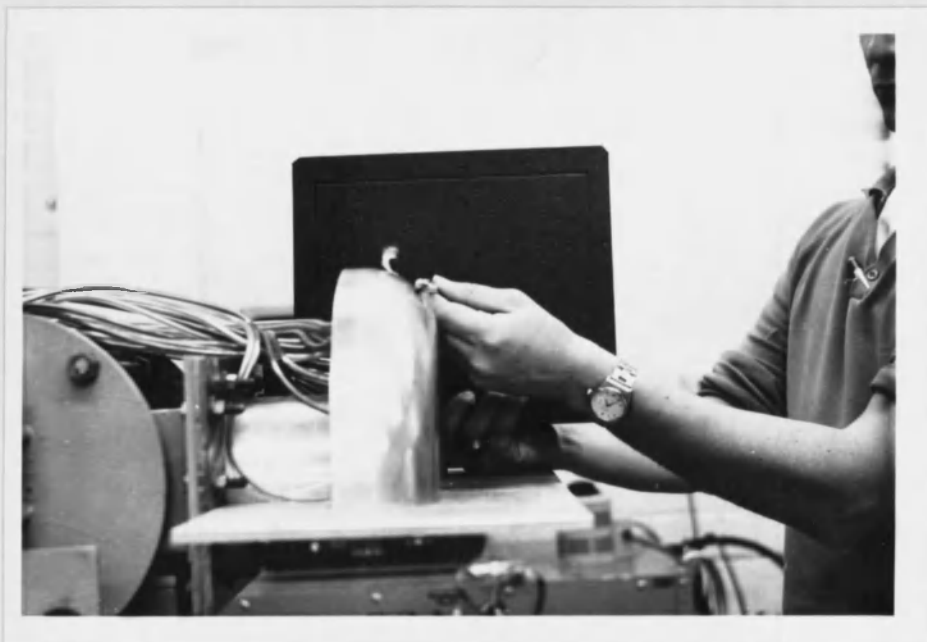


Figure 21. Separation

## CHAPTER IV

### TEST PROCEDURE AND DATA ANALYSIS

#### 4.1 General

The test procedure was designed to be primarily an exploratory type of investigation for possible isolation of areas of interest with practicable application to STOL, VTOL, or thrust reversers. This approach was predicated by the fact that no previous data were available for a Coanda nozzle of this configuration and that best utilization of effort would be obtained by determining promising areas. The information deemed necessary to obtain by testing was:

- 1) Surface pressures at various pressure ratios.
- 2) Jet velocities and thickness of the Coanda sheet.
- 3) Forces produced by the Coanda flow.

#### 4.2 Surface Pressure Distribution

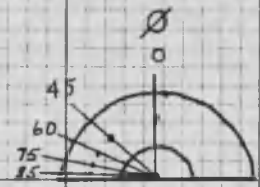
Surface pressures were measured for the nozzle configuration with its full 180 degree turning capability. Pressure ratios (Plenum pressure compared with atmospheric pressure) of 1.02, 1.05, 1.53, 1.60, 1.87, and 2.02 were tested. At the lower pressure ratios, the water manometer

for the surface pressures and the pressure transducer for the plenum pressure were used. At the higher pressure ratios, the mercury manometer was used for both the surface pressures and the plenum pressure. Steady flow conditions were approximated by monitoring the plenum pressure and adjusting the air inlet throttling valve to the desired plenum pressure. This was easily done at the lower pressure ratios, but required closer monitoring at the higher pressure ratios. These pressure ratios encompassed the critical pressure ratio of choked flow at 0.528, or its reciprocal of 1.894.

In the design of the nozzle, a control was provided for a check of uniform flow distribution issuing from the slot. At the 90 degree turning position on the nozzle,  $\theta$  equal 90 degrees, surface pressure ports were drilled at lateral positions of 0, 45, 60, 75, and 85 degrees,  $\phi$  degrees. All of the other ports used for checking the flow at various turning positions were within 45 degrees lateral limits. Figure 22 shows the surface pressure distribution for a constant  $\theta$  equal 90 degrees and varying  $\phi$  degrees for different pressure ratios. Based on the coefficient of pressure, the flow appears uniform within the range of experimental error for the  $\phi$  direction from 0 to 60 degrees. This is assumed to be sufficient justification for using the data from the staggered

$C_{Ps}$   
(-)  
0.04

- $\frac{P_t}{P_{\infty}}$
- = 1.05
  - △ = 1.53
  - = 1.60
  - + = 1.87
  - ◇ = 2.02



0.03

0.02

0.01

0.00

10 20 30 40 50 60 70 80 90  
 $\theta$  DEGREES AT  $\theta = 90$  DEGREES

Figure 22. Surface Pressure Distribution

pressure ports between 0 and 45 degrees lateral limits. The undulation at  $\phi$  equal to 75 degrees is believed to be caused by the proximity of the base plate. This would tend to indicate that near the base plate the uniform distribution of flow is disturbed in this configuration. Gates (6) checked the uniform distribution of flow for a complete axially-symmetric external ejector (no base plate), and found that there was some small variation. This agrees with the results obtained for  $\phi$  between 0 and 60 degrees on the half torus.

Figure 23 depicts the variation of the coefficient of pressure for 28 different stations on the surface. The stations were located by varying  $\theta$  from 0 to 180 degrees. It is noted that for the five pressure ratios used, the negative coefficient of pressure plots into definite groupings. These show definite undulations of pressure on the surface. The strongest undulation is near the nozzle exit. At  $\theta$  equal approximately 120 degrees, the negative coefficient of pressure becomes very weak, and the pressure begins to approach ambient pressure.

von Glahn (24) investigated a curved plate deflection surface, and Bailey (1) investigated a curved plate deflection surface that was separated from the nozzle exit. Both have shown pressure fluctuation that decreased as the length of the deflection surface increased. This

$C_{Ps}$

$\frac{P_c}{P_\infty}$

- 1.05
- △ 1.53
- 1.60
- + 1.87
- ◇ 2.02

0.20

0.10

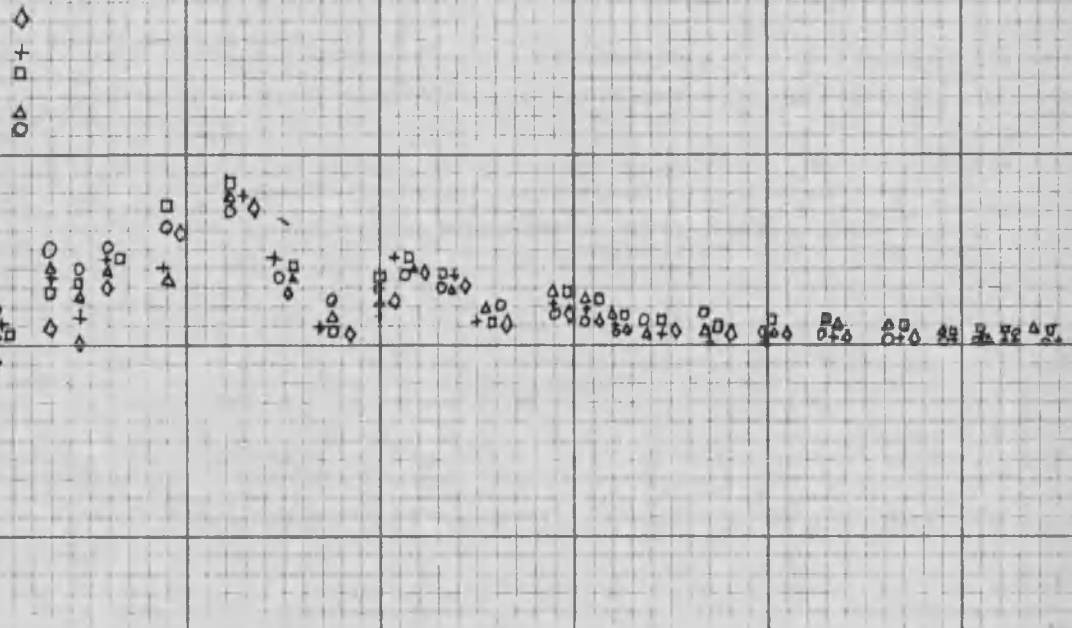
(-)  
0.00  
(+)

0.10

INCHES	1	2	3	4	5	6	7
DEGREES	25.6	51.3	75.9	102.3	128.2	153.8	180.0

DISTANCE MEASURED ON TORUS SURFACE FROM SLOT

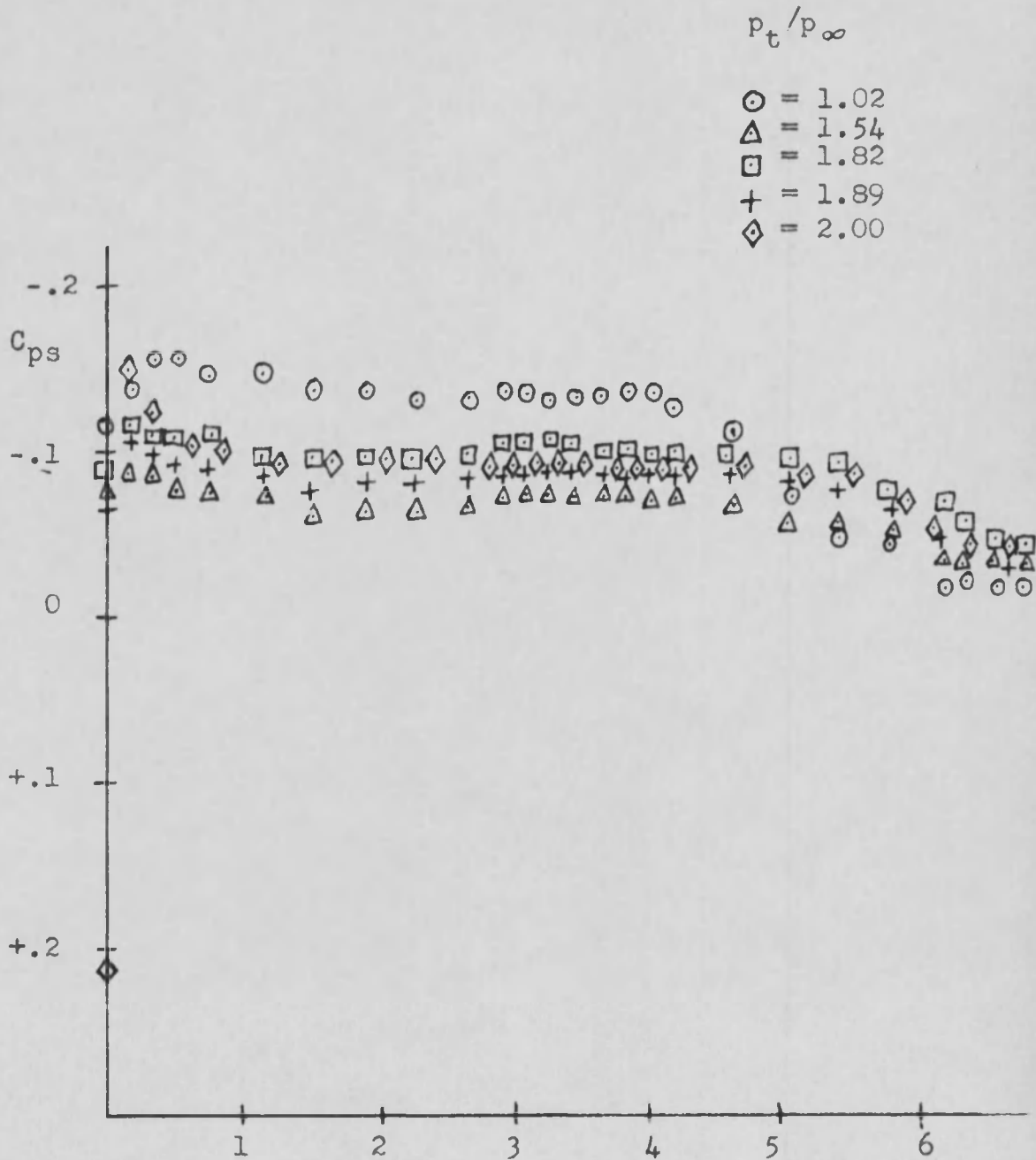
Figure 23. Surface Pressure Distribution,  
 $\phi = 0$  to 45 Degrees



tendency was observed in this study below and above critical pressure ratios. Triner (22) and Palermo (16) found that the pressure fluctuations were of lesser magnitude. The Schlieren photographs presented by Palermo support the correlation of surface pressure variation with expansion and compression of the jet sheet.

A comparison of the flow over the two-dimensional cylinder studied by Palermo (16) and the flow over the three-dimensional half torus with certain geometrically similar parameters shows that the pressure undulations are more pronounced for the half torus, Figures 24 and 23, respectively. Both nozzles produced a positive pressure coefficient at the slot exit at supercritical pressure ratios with the greatest undulation near the exit. The surface pressure approaches ambient pressure with increasing  $\Theta$  for both nozzles. These results tend to agree with Coanda (5) that the "lip" of the nozzle is the active part of the Coanda nozzle.

It is believed that most of the experimental error resulted from reading the manometers during this series of experiments. The manometer readings can be repeated with an accuracy of 0.1 inch of mercury or water. The percentage of error would vary depending on the pressure differential. For the highest pressure differential, it was estimated that the error was approximately 2 per cent.



(Palermo (16) Surface Inches from Slot  
 (Figure 5.5) Pressure Distribution over Cylinder

Surface,  $\theta = 180^\circ$

Figure 24.

### 4.3 Velocities and Thickness of the Coanda Sheet

The investigation of the velocity and thickness of the Coanda sheet was performed by using total and static pressure rakes placed in the jet flow. The rakes were placed at  $\Theta$  positions of 20, 40, 60, 90, 105, and 120 degrees. For the above  $\Theta$  positions,  $\phi$  positions of 0, 45, 60, 75, and 85 degrees were used. The pressure ratio of the ambient pressure to plenum pressure was chosen as 0.977, equivalent to Mach 0.18 at the nozzle exit. This pressure ratio makes the assumption of incompressible flow feasible, and is the same pressure ratio used by Palermo (16) on the cylinder. Air was compressed in the storage tank by the air compressor to a pressure of 120 p.s.i.g. at the beginning of each test. The throttling valve was adjusted to maintain the desired pressure ratio for steady flow. This was easily done because of the amount of stored compressed air available for the small amount needed at this pressure ratio. For each test, the temperature, barometric pressure, and manometer pressures were recorded. Water manometers were used with both the total and static pressure rakes to obtain data for calculating velocities in the Coanda sheet.

Reducing the total and static pressures to velocity was accomplished by Bernoulli's equation for incompressible steady flow.

$$p_{\text{total}} - p_{\text{static}} = \frac{1}{2} \rho v^2$$

$$p = \gamma h$$

$$v = \left( \frac{2\gamma}{\rho} (h_t - h_s) \right)^{\frac{1}{2}}$$

The quantity  $\left( \frac{2\gamma}{\rho} \right)^{\frac{1}{2}}$  can be evaluated separately and used as a constant to obtain the velocity at a point by taking the square root of the difference between the height of water (inches) in the total and static manometers. Further simplification of the formula for conditions of temperature equal 80 degrees F, specific weight of water equal 62.2 pound force per cubic foot, specific weight of mercury equal 846.5 pound force per cubic foot, density of air equal 0.00207 slugs per cubic foot when atmospheric pressure equal 27.3 inches of mercury is:

$$v = 70.8 (h_t - h_s)^{\frac{1}{2}} \text{ ft/sec.}$$

Figures 25 and 26 show Coanda sheet velocity profiles in terms of the height above the torus surface in inches, as determined by Bernoulli's incompressible equation. An attempt to use the data for the case of  $\phi$  equal zero degrees with the apparent fully developed portion of the flow did not show similarity, Figure 27. Similarity was based on the superposition of plots for height above the surface divided by local maximum height, represented

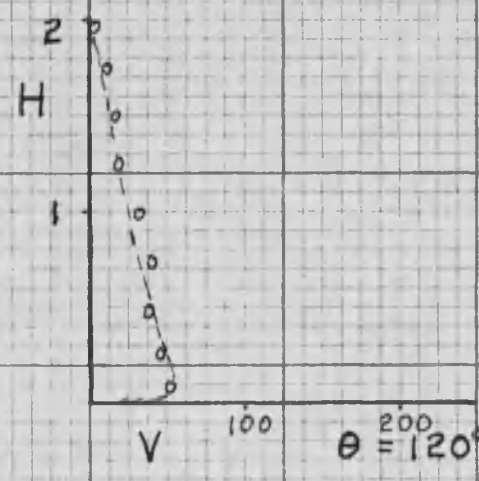
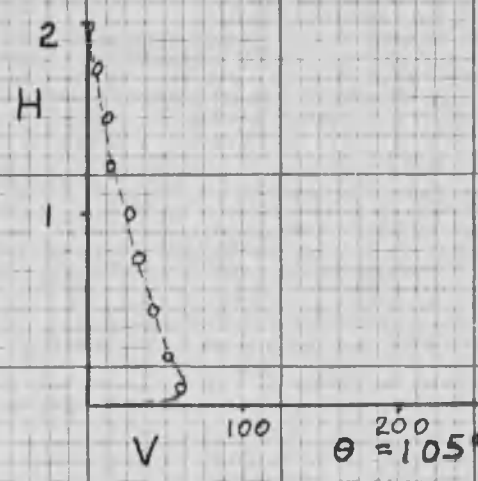
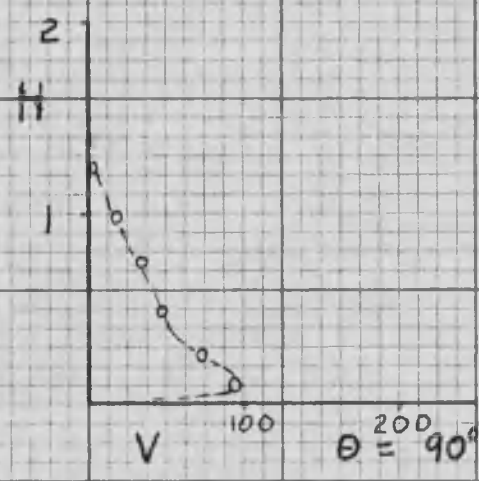
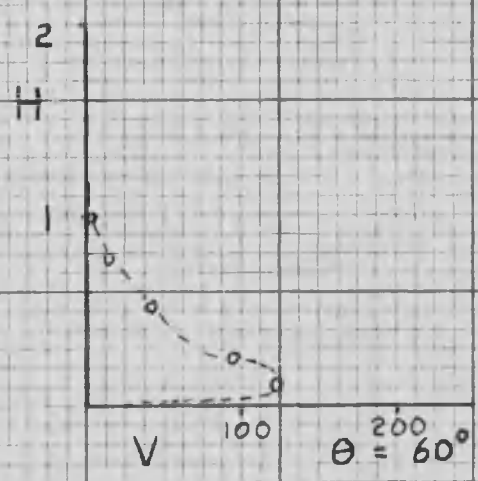
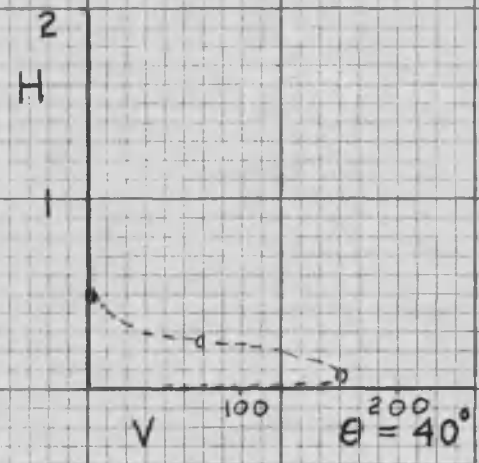
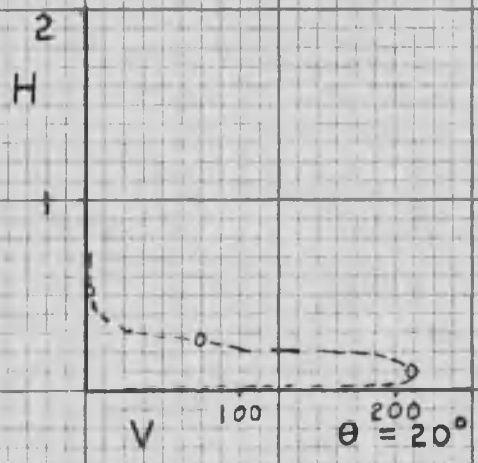
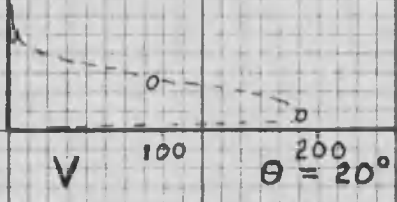


Figure 25. Velocity Distribution,  $\phi = 0^\circ$

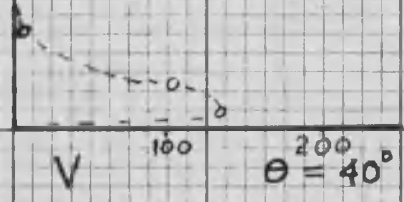
2  
H

1



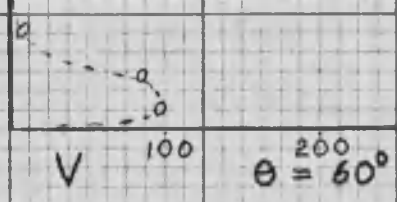
2  
H

1



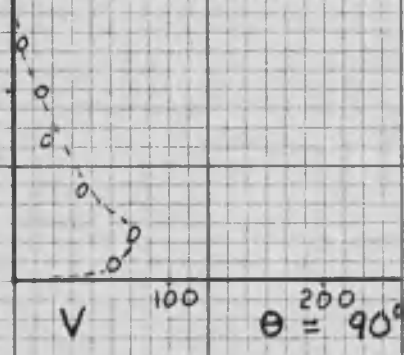
2  
H

1



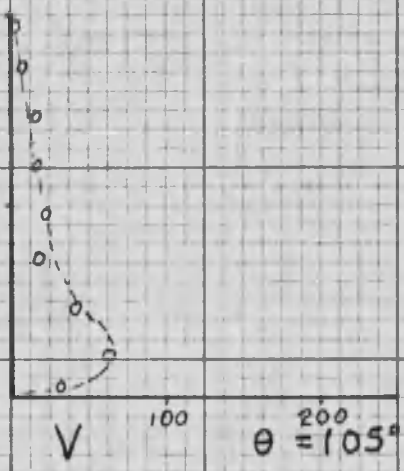
2  
H

1



2  
H

1



2  
H

1

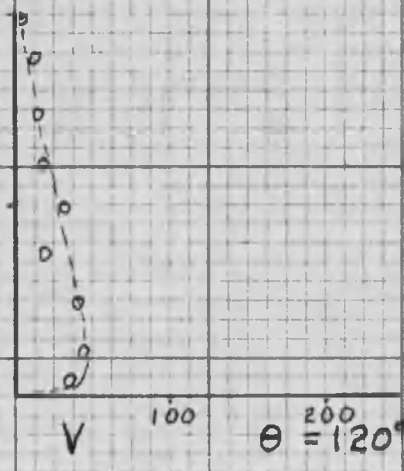


Figure 26. Velocity Distribution,  $\phi = 45^\circ$

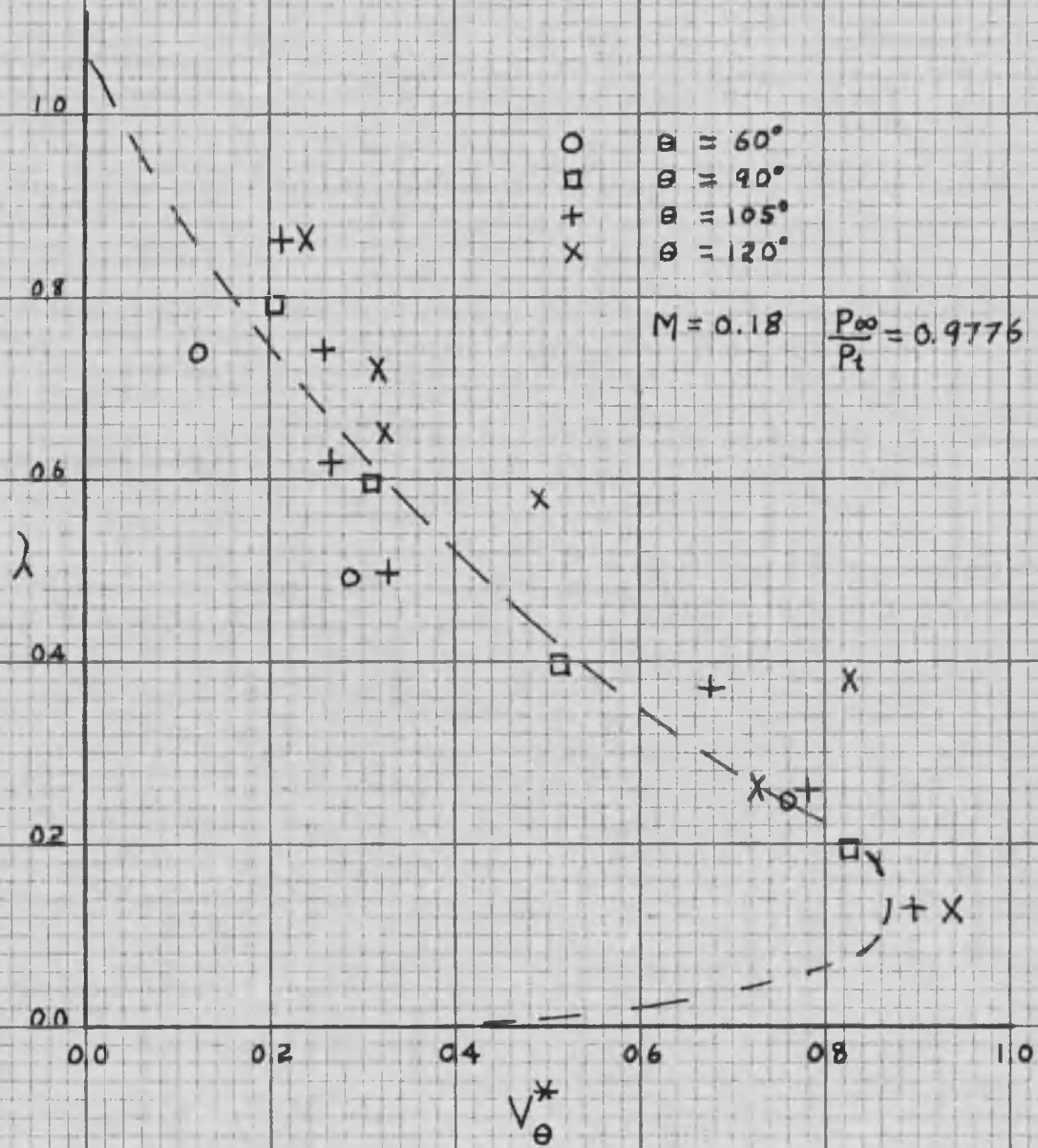
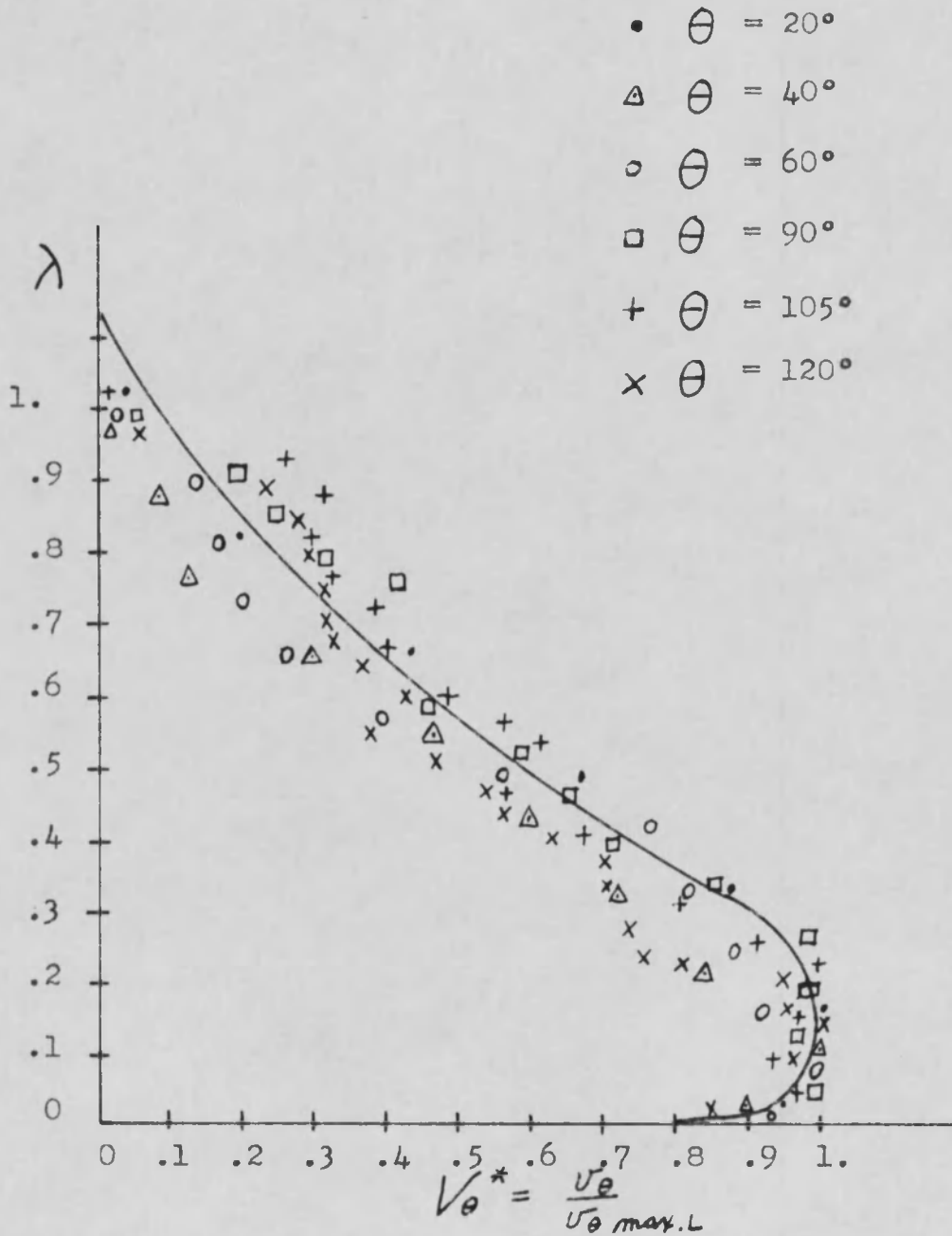


Figure 27. Non-Dimensional Velocity Profile,  $\phi = 0^\circ$

by  $\lambda$ , versus velocity divided by local maximum velocity, represented by  $V_{\theta}^*$ . It is estimated that the maximum flow thickness is approximately 2 inches before the flow begins to lose its ability to cling to the surface. This technique worked very well for Palermo (16) for flow over the cylinder. He was able to show similarity and hence develop equations for the velocity profile in the flow, Figure 28.

A comparison of the velocities at comparable positions on the surface for the half torus and the cylinder reveals that the velocities diminish at a greater rate for the half torus as the flow travels around the surface. This is to be expected due to the additional degree of freedom in the three-dimensional case. Beyond  $\theta$  equal 120 degrees on the half torus the velocity near the surface was too minute to measure, which tends to agree with the coefficient of pressure determined by analyzing the surface pressures.

In Figure 26, flow reversal was indicated at values of 40 degrees and 60 degrees, but is not shown on the plot. This was apparent from the negative pressure coefficients measured at some of the total pressure tubes. A negative pressure coefficient in the total tube could be caused by sufficient change of flow direction to produce a velocity with a large component transverse to the



(Palermo (16)  
 (Figure 5.1) Non-Dimensional Velocity Profile

Figure 28

total pressure tube axis. This tends to support the idea that the flow around the half torus is not a well behaved smooth uniform laminar flow.

Tufts were introduced into the flow at various stations on the surface. At the pressure ratio for Mach 0.18, the flow clung to the surface until past the  $\Theta$  equal 120 degree station. At the  $\Theta$  equal 140 degree station, the tuft was inclined at approximately 40 degrees. This visually shows that the flow has changed in its ability to produce the Coanda effect at this station, Figure 29.

The chief source of error in measuring the velocity is believed to be the misalignment of the total and static pressure rakes with the flow direction. This error obviously would outweigh errors of the pressure transducer or manometer readings.

#### 4.4 Forces Produced by Coanda Flow

The determination of the forces produced on the Coanda nozzle were greatly facilitated by the use of the force balance, the electrical load cells, and the electrical recording instruments. The Baldwin-Lima-Hamilton load cells were calibrated with known forces consisting of weights applied in the horizontal and vertical directions. A linear calibration curve was plotted so that pounds force could be read directly from the curve with a reading

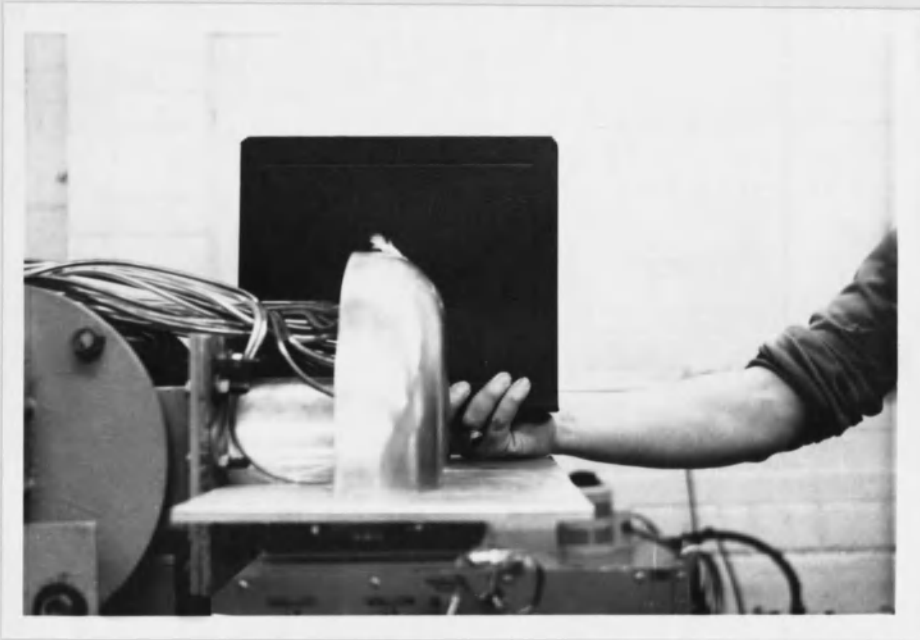


Figure 29. Tuft at  $\theta = 120^\circ$

from one of the recording instruments (Leeds Northrop Potentiometer or X-Y Recorder). A known resistance was placed in the circuit which produced a reading on the recording instruments. This reading was plotted on the calibration curve and used as a reference point for checking the calibration curve at later dates. In this manner, the task of calibrating the load cells each time an experiment was conducted was not necessary. A linear calibration curve was also prepared for the 15 p.s.i.g. Statham Pressure Transducer, and a known resistance superimposed on the curve.

The air bearings on each side of the plenum were adjusted to 0.004 inch clearance, and air pressure for the bearings was adjusted to 10 p.s.i.g. In the determination of forces, it was found necessary to frequently check the air bearings to insure that no physical contact existed between bearing surfaces.

The conduct of the test procedure was based upon three turning angles of  $\theta$  equal to 0, 90, and 180 degrees. For each of the turning angles, six pressure ratios (total plenum pressure divided by ambient pressure) of 1.52, 1.66, 2.00, 2.25, 2.52, and 2.61 (reciprocals equal 0.658, 0.601, 0.500, 0.440, 0.397, and 0.383, respectively) were tested. The pressure ratio was maintained by manually adjusting the throttling valve. The test data were recorded by the

electrical recording instruments; the X-Y Recorder recorded the plenum pressure and the vertical force, while the Potentiometer recorded the horizontal force.

In the analysis of this test, it was desired to determine if a high turning efficiency with force augmentation could be realized. The most direct experimental approach to this problem appeared to be determining the turning efficiency by comparison of forces. The forces to be compared were produced as a result of the flow turning through 0, 90, and 180 degrees. Six different pressure ratios were used for each of the three different magnitudes of flow turning, but the exit area remained constant. The turning of the flow was limited to zero and ninety degrees by using deflectors. For the turning of the flow through 180 degrees, no deflector was required. The forces obtained with the turning of the flow limited to zero degrees,  $\theta$  equal to zero degrees were determined.

It was found that the forces consisted of an upward vertical force of 20 to 25 per cent of the total resultant force, over the range of pressure ratios used. The total resultant force at  $\theta$  equal to zero degrees was used as a basis of comparison in order to determine the turning efficiencies. For example, the horizontal and vertical force components were measured for the flow turning ninety degrees, and their total resultant force was calculated.

Each of the measured force components and their total resultant force was divided by the total resultant force for the turning of the flow limited to zero degrees. The quotient was reported as turning efficiency,  $\eta$ .

The turning efficiencies for the vertical component, horizontal component, and the total resultant force for  $\theta$  equal to 90 and 180 degrees are shown by Figures 30 and 31, respectively. Neither of these graphs showed any flow augmentation where the efficiency is greater than 100 per cent. The highest efficiency obtained was 96 per cent for the total resultant  $\eta_T$  with  $\theta$  equal to 90 degrees at a pressure ratio of 0.601. Although not shown, it is worthy to note that at  $\theta$  equal to 0 degrees, the vertical forces were equivalent to a force acting upward, and for  $\theta$  equal to 90 and 180 degrees the vertical forces were equivalent to a force acting downward. The horizontal forces were equivalent to a force acting opposite to the exit flow direction for  $\theta$  equal to 0 and 90 degrees, whereas, for  $\theta$  equal to 180 degrees the equivalent force was reversed. Since the flow at  $\theta$  equal 180 degrees produces a horizontal force that is in the same direction as the original exit flow and a vertical force that acts downward, the resultant flow may have practical application.

Numerous investigators working with two-dimensional nozzles, analogous to flow over a cylinder, have reported

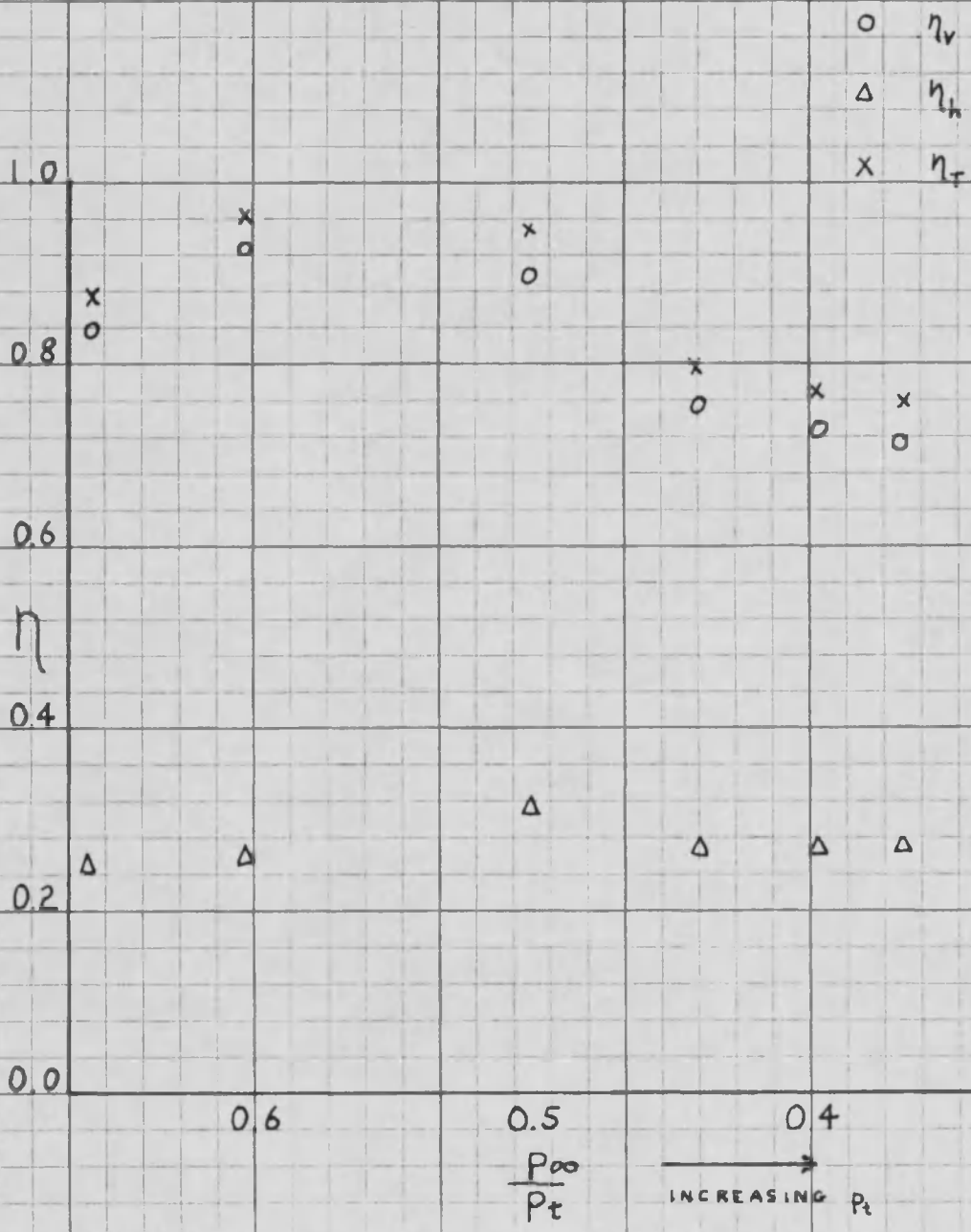


Figure 30.  $\Theta = 90^\circ$ , Turn Efficiency ( $\eta$ ) vs. Pressure Ratio

$$\eta_v = \frac{F_v}{F_0}$$

$$\eta_h = \frac{F_h}{F_0}$$

$$\eta_T = \frac{F_T}{F_0}$$

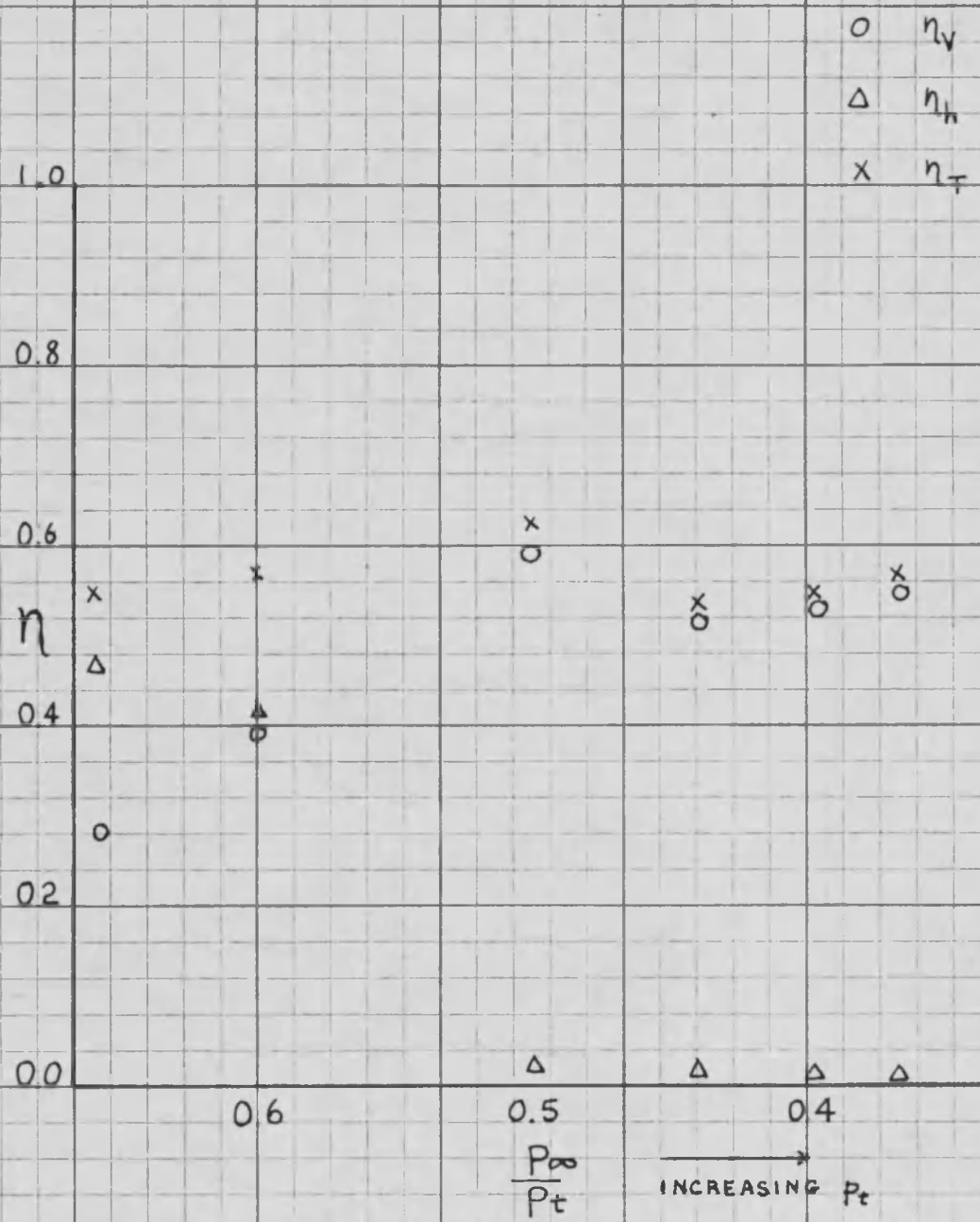


Figure 31.  $\Theta = 180^\circ$ , Turn Efficiency ( $\eta$ ) vs. Pressure Ratio

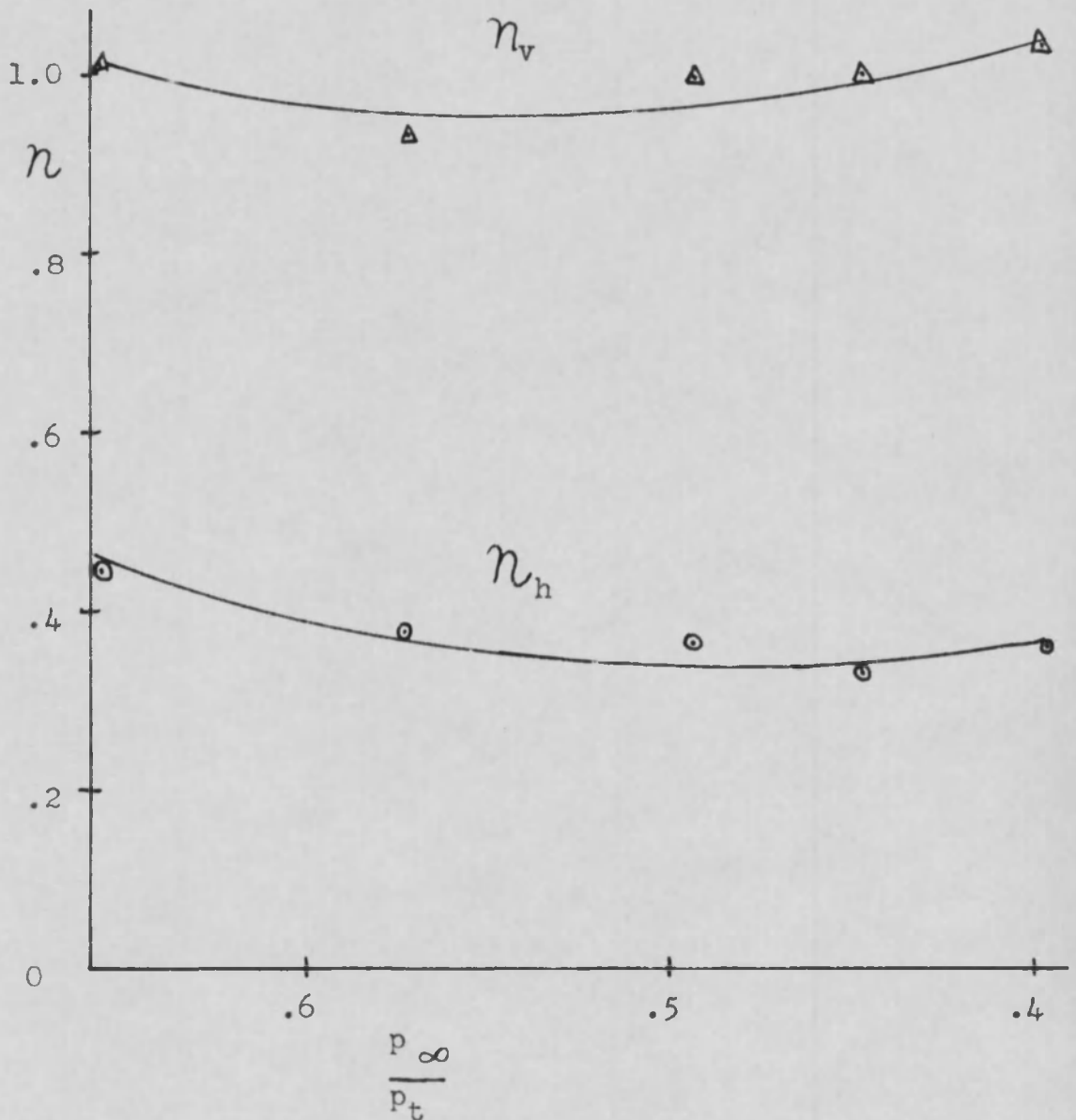
$$\eta_v = \frac{F_v}{F_0}$$

$$\eta_h = \frac{F_h}{F_0}$$

$$\eta_T = \frac{F_T}{F_0}$$

high turning efficiencies for the vertical component with  $\theta$  equal to 90 degrees. von Glahn (24) reports 81 per cent for a ratio of vertical component (lift) to undeflected thrust; Bailey (1), using a theoretical thrust equation, obtained 90 per cent; Triner (22) also on the basis of a theoretical thrust equation obtained 89 per cent, but when he evaluated on the basis of measured vertical component (lift) to measured thrust,  $\theta$  equal to zero, he obtained 97 per cent; Palermo (16), using the same criteria of measured thrust for comparison, reports 100 per cent at a pressure ratio of 0.658, ambient pressure versus total plenum pressure.

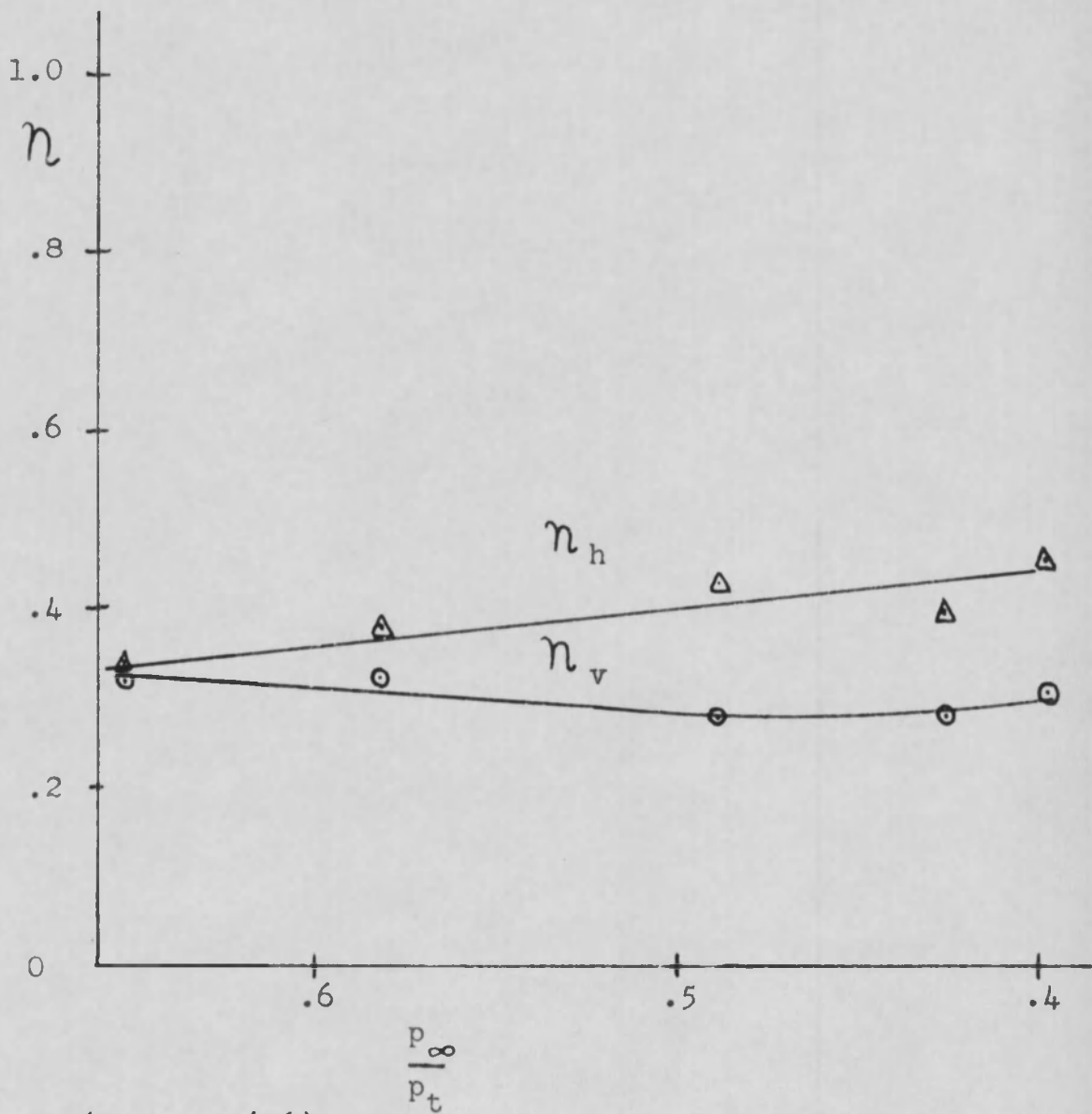
The nozzle, consisting of a cylinder with two-dimensional flow, used by Palermo, had geometrical parameters that were similar to the half torus. It is interesting to compare the turning efficiencies by referring to Figures 30 and 31 versus Figures 32 and 33 reported by Palermo. It appears that the two-dimensional flow over the cylinder has a higher turning efficiency for both the vertical component and the horizontal component than three-dimensional flow over the half torus, when  $\theta$  is equal to 90 degrees. When the turning efficiencies are considered for  $\theta$  equal to 180 degrees, the half torus appears to be more efficient than the cylinder. This is probably caused by the tendency of the flow to separate from the half torus



(Palermo (16)  
 (Figure 5.8) Turn Efficiency ( $n$ ) vs Pressure Ratio at  
 $\theta = 90^\circ$

$$n_v = \frac{F_v \text{ (measured at } 90^\circ\text{)}}{F \text{ (measured at } 0^\circ\text{)}}, \quad n_h = \frac{F_h \text{ (measured at } 90^\circ\text{)}}{F \text{ (measured at } 0^\circ\text{)}}$$

Figure 32



(Palermo (16)  
 (Figure 5.9) Turn Efficiency ( $n$ ) vs Pressure Ratio at  $\theta = 180^\circ$

$$n_v = \frac{F_v \text{ (measured at } 180^\circ\text{)}}{F \text{ (measured at } 0^\circ\text{)}}, \quad n_h = \frac{F_h \text{ (measured at } 180^\circ\text{)}}{F \text{ (measured at } 0^\circ\text{)}}$$

Figure 33

after 120 degrees of turning, whereas, the tendency of the flow to separate from the cylinder was not observed by Palermo over the range of pressure ratios tested.

It would appear by observing Figures 30 and 31 for the half torus that most of the vertical force component is produced during the first 90 degrees of turning. Figure 31 for  $\theta$  equal 180 degrees, shows a sudden decrease in the efficiency of turning for the horizontal force component. This could indicate that the flow separates as the plenum pressure is increased, but only after sufficient turning to produce a relatively strong vertical component compared to the horizontal component.

Gates (6) in his comparison of the Coanda flow for a three-dimensional and a two-dimensional model, was unable to find any significant difference in the performance based on ideal thrust ratio. He was unable to show any static thrust augmentation with the external type ejector. The present study would tend to agree with Gates. The flow over the three dimensional half torus apparently does not show any significant improvement of flow augmentation, when compared with the flow over the two-dimensional cylinder.

The experimental error associated with the force measurements are assumed to be negligible, for an exploratory investigation, when considering the electrical apparatus used, due to the high order of reproducibility of data.

Probably the greatest error resulted from the manual control of the throttling valve in an effort to obtain steady flow. The pressure ratio is considered to be accurate within approximately 5 per cent for the steady flow conditions.

## CHAPTER V

### CONCLUSIONS

#### 5.1 Conclusions

The primary conclusion reached in the present exploratory type investigation is that no substantial force augmentation with high turning efficiency of either the vertical, horizontal, or total resultant force is produced with this particular nozzle (three-dimensional, half torus, external ejector), over the range of pressure ratios tested from 1.52 to 2.61. The highest turning efficiency obtained was 96 per cent, for the total force resultant ( $\eta_T$ ), when  $\Theta$  was equal to 90 degrees at a pressure ratio of 0.601. The vertical force component was the predominant force compared with the horizontal force component (3.65 to 1.00).

Based upon the data obtained by measurements from the surface pressure ports and velocities in the Coanda jet sheet, the flow can be considered to be uniform laterally from  $\phi$  equal 0 to 60 degrees. Pronounced surface pressure undulations were recorded over the entire range of pressure ratios tested. At supercritical pressure ratios, there was a positive pressure coefficient at the throat of the exit.

With the incompressible flow assumption applied to Bernoulli's equation at Mach 0.18, the velocity profiles in the axial planes for fully developed flow were not similar. The flow exhibited properties of separation, reduced surface pressure gradient and no measurable tangential velocity, past 120 degrees of turning. Before the separation properties were apparent, the jet sheet thickness was approximately 2 inches.

The turning efficiency of the flow for  $\theta$  equal to 180 degrees was less than for  $\theta$  equal to 90 degrees. The highest turning efficiency,  $\eta_T$  equal to 63 per cent when  $\theta$  equal to 180 degrees, was obtained at a pressure ratio of 0.50. The vertical force component was the predominant force compared with the horizontal force component (3.14 to 1). The turning efficiency of both the vertical and the horizontal force components were sufficiently reduced to render their utility doubtful.

The particular three-dimensional nozzle of this study offers no obvious substantial advantage over the two-dimensional nozzle with geometric similar parameters studied by Palermo (16).

The test apparatus consisting of the force balance, common plenum with air bearings, and electrical measuring instruments does offer an expeditious direct method of

obtaining data for future investigations with minimum calculations.

## 5.2 Recommendations for Further Research

The literature pertaining to the "Coanda effect" and its various modifications is becoming very voluminous. No doubt, if a substantial flow augmentation with high turning efficiency were obtained and used for a practical application, the research work on "Coanda effect" would receive added stimulus and the literature would greatly multiply.

At the present time, it appears that a most worthwhile study and contribution would be an exhaustive, systematic literature research on the "Coanda effect." Numerous investigators have studied the "Coanda effect" and have isolated parameters that they believed would enhance flow augmentation. Parameters such as nozzle exit overhang, ratio of slot width and height, radius of curvature for a curved deflection surface, smoothness of surface, pressure ratios, the gap associated with ventilated clinging flow, and many others could be studied and their effects tabulated. Future investigators could use a study of this nature as a departure point in an effort to put together a combination of parameters that would give the desired substantial increase in flow augmentation. Chang (14) reviewed 31 articles pertaining to "Coanda effect."

His review is very useful; however, emphasis does not appear to be on determining the significant parameters for flow augmentation with high turning efficiency.

Once the combination of parameters for a substantial optimum flow augmentation can be determined, then the application of the principle to STOL, VTOL, thrust reversers, etc., would naturally follow.

## REFERENCES

1. Bailey, A. B. "Use of the Coanda Effect for the Deflection of Jet Sheets over Smoothly Curved Surfaces," UTIA Tech Notes No. 49, Univ. of Toronto, Aug. 1961.
2. Boyer, E. J. "Preliminary Investigation and Evaluation of the Coanda Effect," Tech Rpt No. F-TR-2207-ND ATI No. 26895, Aug. 1948.
3. Bourque, C., and Newman, B. G. "Reattachment of a Two-Dimensional Incompressible Jet to an Adjacent Flat Plate," The Aeronautical Quarterly Review. V. XI Aug. 1960.
4. Chang, P. K., "Survey on Coanda Flow," O.N.R. Contract Nonr-2747(00), 1963.
5. Coanda, H. "Analysis of Thrust Due to the Coanda Phenomenon," Tech Rpt Contr Nr AF 61-(052), Oct. 1960.
6. Gates, M. F. "Static Lift Characteristics of Jet Slots, a Clarifying Study of the External Ejector," Hiller Acft Corp Rpt No. ARD 213, AD 218849, Oct. 1958.
7. Gates, M. F. "Investigation of Ventilated Clinging Flow Phenomenon," Hiller Acft Corp Rpt No. ARD-311, AD 420838, Aug. 1963.
8. Hughes, W. F., and Gaylord, E. W. "Basic Equations of Engineering Science," Schaum Publishing Company, 1964.
9. Korbacher, G. K. "The Coanda Effect at Deflection Surfaces Detached from the Jet Nozzle," Canadian Aeronautics and Space Journal Vol 8 No. 1, Jan. 1962.
10. Levin, S. G., and Manion, F. M. "Jet Attachment Distance as a Function of Adjacent Wall Offset and Angle," TR-1087, Dec. 1962.
11. Liepmann, H. W., and Roshko, A. "Elements of Gas-dynamics," John Wiley and Sons, Inc., 1962.

12. Marwood, R. M. "An Experimental Investigation of Coanda Effect," Thesis Project No. M-156, Contract No. 33-038-ac-17625, Purdue Univ. Experiment Station, 1949.
13. Metral, A. R. "Methods of Increasing Fluid Stream by Diverting it from its Axis of Flow, Coanda Effect," ATI 18883, 1939.
14. Moon, P., and Spencer, D. E. "Field Theory for Engineers," D. Van Nostrand Co., Inc., 1961.
15. Pai, Shih-I. "Fluid Dynamics of Jets," D. Van Nostrand Company, Inc., 1954.
16. Palermo, F. J. "An Investigation of the Two-Dimensional Coanda Effect," Thesis, Dept. of Aerospace Engineering, Univ. of Arizona, 1965.
17. Roderick, W. E. "Use of the Coanda Effect for the Deflection of Jet Sheets over Smoothly Curved Surfaces," UTIA TN No. 51, Univ. of Toronto, Sept. 1961.
18. Schubauer, G. B. "Jet Propulsion with Specific Reference to Thrust Augmenters," U. S. Bureau of Standards, NACA TN 442, Jan. 1933.
19. Sproule, R. S., and Robinson, S. T. "The Coanda Effect," ATI 60505, Date Unk.
20. Sridhar, K. "An Experimental Investigation of the Flow in and behind Two-Dimensional Jet Sheets Bounding a Cavity," KTIA Reprt No. 94, Aug. 1963.
21. Sterne, L. H. J. "Analysis of Thrust Due to the Coanda Phenomenon," Tech Rpt to A.R.D.C., Jan. 1961.
22. Triner, E. G. "An Experimental Investigation of the Coanda Phenomenon," Thesis, Dept. Aerospace Engineering, Univ. of Arizona, 1963.
23. Voedisch, A. "Analytical Investigation of the Coanda Effect," Proj. No. FP-188, Tn Rpt No. TR 3155 ND, April 1947.
24. von Glahn, U. "Use of the Coanda Effect for Jet Deflection and Lift with a Single Flat-Plate and Curved-Plate Deflection Surface" NACA TN 4377, Sept. 1958.

25. von Glahn, U. "Use of the Coanda Effect for Jet Deflection and Vertical Lift with Multiple-Flat-Plate and Curved-Plate Deflection Surfaces," NACA TN 4377, Sept. 1958.
26. von Karman, T. "Theoretical Remarks on Thrust Augmentation," Memorial Dinner, Cal Tech.
27. Yen, K. T. "A Theoretical Evaluation of the Coanda Nozzle," TR AE 5501, Rensselaer Poly Inst., July 1955.